DOCUMENT NO. 67SD4388
29 SEPTEMBER 1967

FINAL REPORT

MEASUREMENT OF THERMAL CONDUCTANCE OF MULTILAYER AND OTHER INSULATION MATERIALS

BY

ERWIN FRIED
GILBERT S. KARP
ROBERT B. HOBBS
GERALD HIESER

PREPARED FOR

CREW SYSTEMS DIVISION
NATIONAL AERONAUTICS AND SPACE ADMINISTRATION
MANNED SPACECRAFT CENTER
HOUSTON, TEXAS

CONTRACT NAS 9-3685

GENERAL ELECTRIC

SPACECRAFT DEPARTMENT
A Department of the Missile and Space Division
Valley Forge Space Technology Center
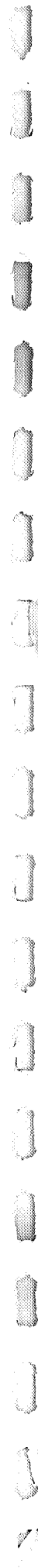P. O. Box 8555 ● Philadelphia, Penna. 19101

TABLE OF CONTENTS

LIST OF ILLUSTRATIONS

ACKNOWLEDGEMENTS

SECTION 1

INTRODUCTION

This report presents the results of a primarily experimental program, concerned with the performance of multilayer thermal insulation used in spacesuits, under varying environmental conditions such as temperature extremes and degree of compression.

The program was divided into two distinct tasks:

> Task 1 – consisting of thermal conductance measurements of aluminized polyester films, in vacuum, with varying numbers of layers for a fixed thickness of insulation.

> Task 2 – consisting of thermal conductance evaluation, on a parametric basis, of NASA furnished space suit assembly material samples. Significant variables were compression of the multilayer layups and boundary temperatures.

Both tasks included supporting analysis and suggestions for improvements of thermal performance, if, and where, practicable.

The reporting period for this work extends from March 21, 1966 through September 30, 1967.

1.1 OBJECTIVES

This program was undertaken to obtain thermal performance data on the extravehicular spacesuit garment material.

Task 1 – the initial phase of the program, was a basic investigation of the effect on thermal conductance of numbers of layers, and degree of compression for crinkled aluminized polyester films, separated by nonwoven Dacron. The number of film layers ranged from 2 to 9 for a fixed sample thickness.

This was followed by Task 2, the experimental evaluations of the thermal conductance of a number of spacesuit layups with different types of materials, spacers, etc. for varying compressions. The boundary temperatures were varied from -320°F to $+285^{\circ}$F, with the body-side temperature held at about 70°F in all cases.

A major change in insulations to be evaluated took place when essentially new material assemblies, consisting of high combustion resistant constituents, were introduced in the latter stages of this program. This work continued for the remainder of the contract period.

All test data reported are based on experiments performed at steady-state conditions. For this reason the testing program on the multilayer layup combinations was performed on a full-time, continuing basis, since considerable time elapsed before steady-state conditions were achieved. During the course of the program, improvement in test procedures, data acquisition and updating of equipment was a continuing effort. Such improvements or changes are discussed in the appropriate section of this report.

1.2 CONCLUSIONS

Since the program covered by this report is divided into Tasks 1 and 2, the conclusions must be divided in a similar manner.

1.2.1 TASK 1 CONCLUSIONS

On the basis of results obtained in Task 1, it can be concluded that there exists an optimum insulation density for the samples tested, but this applied only for the thickness tested. This optimum is 5-6 layers (or 80-90 layers per inch) for the low temperature case and 7-8 layers (110-120 layers per inch) for the high temperature case. Thus, the choice of 7 layers is an average optimum, if the thickness assumed was representative of spacesuit conditions.

It is desirable that a program similar to that of Task 1 be repeated for the new insulation materials currently considered. If there is not enough time, then the "brute force" optimization of checking actual layups appears as a desirable approach, provided past experience is utilized.

1.2.2 TASK 2 CONCLUSIONS

On the basis of the work performed under this task the following conclusions appear reasonable:

a. The thermal performance of aluminized Mylar - nonwoven Dacron insulation appears to be better than that of the aluminized Kapton - beta glass insulation, under compression. However, since the latter insulation constituents are thicker, performance should be equal if this thickness effect is considered.

b. Effort should be applied to improve the degree and quality of the crinkling of the aluminized film used in this program since this crinkling provides the insulation separation.

c. The effect of compression on the thermal performance of multilayer insulations can be compared to that of contact conductance of solids and should be amenable to analysis similar to that of contacts.

d. There appears to be no significant thermal advantage in using beta glass marquisette for insulation spacer material over lightweight beta glass cloth.

e. The effect of residual gas at 5 psia (nitrogen, oxygen) on the thermal performance of the insulation tested appears to be greater than that due to the gaseous conduction contribution alone.

f. The effects of moisture combined with elevated temperature on the stability of the aluminum film in multilayer insulation, as used in spacesuits, may be a problem, since it has been found to be a problem in spacecraft insulation work performed at GE (Ref. 7).

1.3 RECOMMENDATIONS

The following recommendations, based on the reported and related insulation work, are made:

a. Perform additional experimental work to achieve an insulation having better thermal performance at high insulation compression. This should include extensive experimentation supported by some analytical work.

b. Investigate the need for additional and better crinkling of the aluminized film.

c. Perform thermal conductance experiments on a parametric basis to establish the suitability of alternate spacer material.

d. Investigate the effect of residual gas pressure on insulation thermal performance from vacuum to 5 psia pressure.

e. Evaluate the effect of insulation perforations on the thermal performance of such insulation.

f. Evaluate the effect of controlled spacesuit gas leakage on the thermal performance of insulation.

g. Investigate the possible deleterious effect of trapped moisture on the multilayer insulation in the spacesuit.

SECTION 2

DISCUSSION AND RESULTS

This section of the report presents a discussion of the approaches, as well as the results, of the multilayer insulation testing program. Since the program was carried out in discrete tasks, the results will be presented in that order.

Figure 2-1 shows schematically the insulation layups which have been evaluated in this experimental program. The test apparatus and test procedures are discussed in Section 3. All tests, except one at 5 psia environmental pressure, which is discussed separately, were performed in vacuum under steady state conditions. Vacuum is defined herein as an ambient pressure of 10^{-5} mm Hg or lower.

TASK 1

NYLON FELT
HT-1 NYLON
INSULATION
HT-1 NYLON
NYLON FELT

2 TO 9 LAYERS OF 1/4 MIL ALUMINIZED (1 SIDE) CRINKLED POLYESTER FILM (NRC-2), SEPARATED BY NONWOVEN DACRON

TASK 2A

2 LAYERS RUBBERIZED CLOTH
INSULATION
HT-1 NYLON

7 LAYERS 1/4 MIL ALUMINIZED (1 SIDE) CRINKLED POLYESTER FILM (NRC-2), SEPARATED BY 5 LAYERS NONWOVEN DACRON AND 2 LAYERS NYLON MARQUISETTE

TASK 2B

RUBBERIZED CLOTH
BLUE NYLON CLOTH 603
2 LAYER BLADDER CLOTH
INSULATION
2 LAYER BETA GLASS CLOTH

7 LAYERS 1/2 MIL ALUMINIZED (2 SIDES) CRINKLED KAPTON, SEPARATED BY 6 LAYERS OF BETA GLASS CLOTH

TASK 2C

BLADDER CLOTH
BLUE NYLON
2 LAYER BLADDER CLOTH
INSULATION
2 LAYER BETA GLASS CLOTH

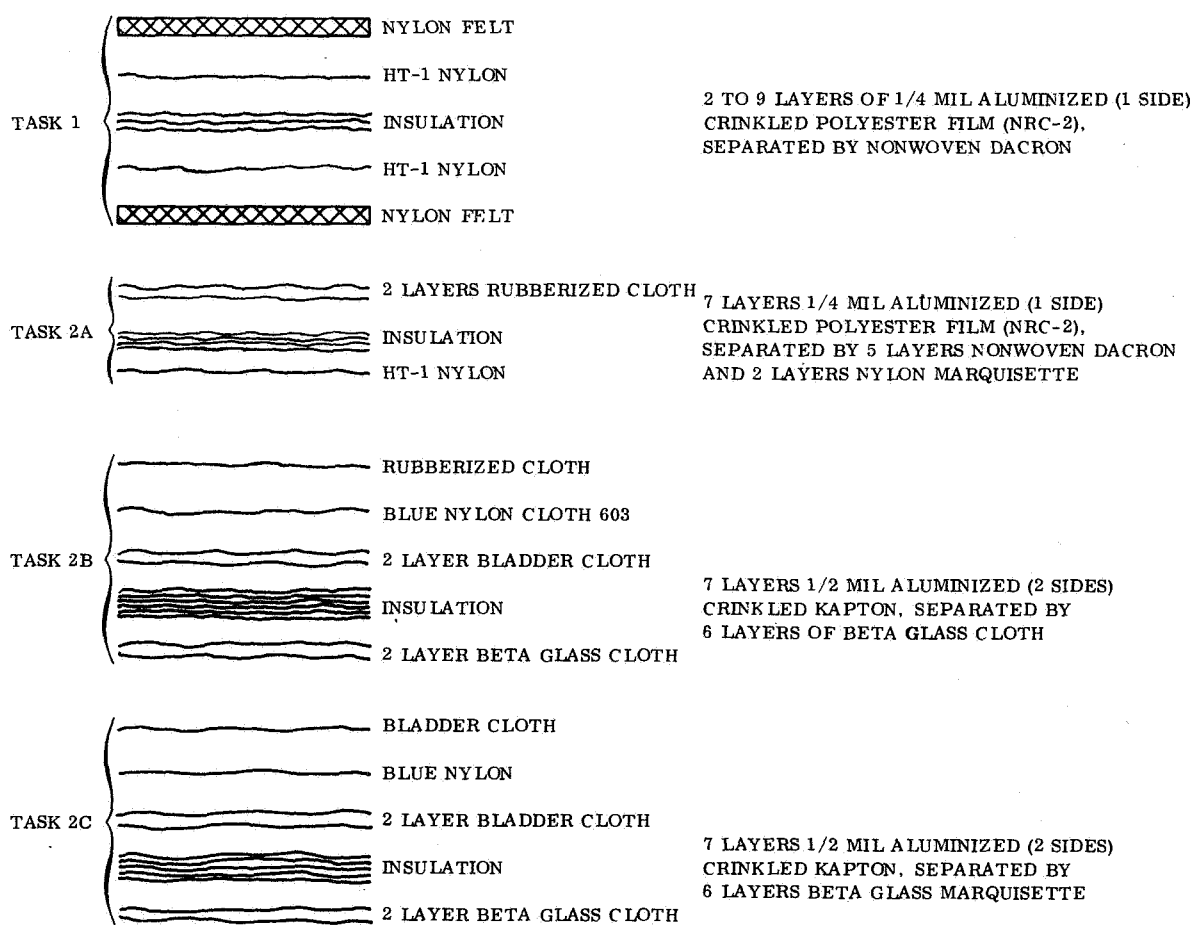7 LAYERS 1/2 MIL ALUMINIZED (2 SIDES) CRINKLED KAPTON, SEPARATED BY 6 LAYERS BETA GLASS MARQUISETTE

Figure 2-1. Schematic of Insulation Layups

2.1 TASK 1

2.1.1 TASK 1 DISCUSSION

The primary objective of the experimental work performed in this task has been to determine the effect of varying the number of layers of aluminized polyester film and nonwoven Dacron spacers for a given overall sample thickness on the overall insulation thermal conductance.

Also, an attempt was made to determine whether heating the same multilayer insulation layup repeatedly would result in "ironing out" the initial crinkling which is necessary for layer separation. Such flattening of the polyester film would result in increased contact conductance through the insulation and, consequently, higher thermal conductivity. A further item of interest has been the possible hysteresis effect of alternate heating and cooling of the test sample.

The test sample and component details are shown in Figure 2-2.

NYLON FELT

MULTILAYER INSULATION   HT-1 NYLON

          HT-1 NYLON
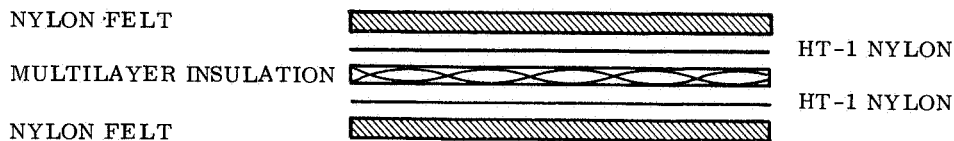
NYLON FELT

MATERIAL SPECIFICATIONS

TRADE NAME		OTHER SPECIFICATIONS	SUPPLIER
100% NYLON FELT	62-NY8/125	1/8 IN. THICK, 8 OZ/YARD, 68 IN. WIDE	AMERICAN FELT CO.
HT-1 NYLON (NOMEX)	ACS-2246	188 x 96 COUNT, 4 OZ/YARD	DAVID CLARK CO.
MULTILAYER INSULATION	----	1/4 MIL Al MYLAR (ALUMINIZED ONE SIDE) VARIABLE NUMBER OF SHEETS	NASA-MSC
	----	2 MIL NONWOVEN DACRON	NASA-MSC

Figure 2-2. Test Sample and Component Details

The inclusion of the 1/8-inch thick-nylon felt in the sample layup was necessary to permit use of the guarded hot plate test apparatus without introducing excessive potential errors. If, for example, 4 layers of "as received" crinkled 1/4 mil aluminized polyester film and Dacron spacers stack up to about 0.040 inch thickness, to which is added about 0.010 inch for the other items, the total sandwich thickness is not more than about 0.050 inch. If the test apparatus hot and cold plates were perfectly flat and in perfect alignment, the potential error in sample thickness or spacing determination would be about 3 mils, which is 6% of the total thickness. Since, the plates are not perfectly flat, and over a 15 inch sample area the alignment is not perfect, the potential thickness error would be a significant portion of the overall 0.050 inch sample thickness. A further problem would have been the determination of the initial sample thickness, if only the polyester film-Dacron spacer spacer insulation had been used.

In order to obtain data of potential value for space suit thermal insulation application, the following approach was taken. The insulation of interest was sandwiched between layers of HT-1 (Nomex) nylon and this in turn was sandwiched between layers of 1/8 inch thick, but resilient nylon felt. It was reasoned that this would permit testing the insulation under conditions approximating those in a space suit assembly, while permitting interpretation of data with reasonable accuracy. Furthermore, the effective thermal conductance of the nylon felt could be measured independently and factored into the data analysis.

It was observed, experimentally, that a total sample sandwich thickness of 5/16 inch provided a snug fit of the insulation between the heating and cooling plates of the test apparatus. For this reason, the 5/16 inch thickness was selected for all Task 1 tests.

2.1.2 TASK 1 RESULTS

Table 2-1 shows the summary of test data, however, not in the order of performance of these tests. The samples were tested under two test conditions:

a. Hot case- $T_h = 300^{\circ}F$, and Tc $= 70^{\circ}F$

b. Cold case- $T_h = 70^{\circ}F$, $T_c - 320^{\circ}F$

Figure 2-3 shows this data graphically for all 23 test points, in the form of effective thermal conductivity vs number of layers of aluminized polyester. In this plot all test data points are given equal weight, although some hysteresis effects are present and certain data points (3.1, 4.1, 5.1) are doubtful. Figure 2-4 shows the same data but weighted in favor of data points in which we have more confidence. The resulting optimum number of layers appears to be the same in both figures.

The minimum effective thermal conductivity falls at about 5-6 layers of aluminized Mylar at the lowest temperature conditions and between 7 and 8 layers of aluminized Mylar for the higher temperature tests. Whether these optimum points are the optimum in an actual suit layup (noting the effect of stitching and local compression) needs verification by testing an actual suit.

Since the nylon felt was added to the test as an expedient, and we were really interested in the thermal performance of the multilayer insulations only, the following approach was used to determine the effect on thermal conductivity of the number of layers of aluminized film without the felt.

The thermal conductivity of the two layers of nylon felt was measured without multilayer insulation. This data is shown as runs 9.1 and 9.2 in Table 2-1. The felt was inserted in the test apparatus at a thickness of 1/4 inch, which provided a snug fit, similar to that with the multilayer insulation. These tests were performed at the same boundary temperatures as before, since the felt was in direct contact with the boundary plates in both cases.

Table 2-1. Task 1 Test Data Summary

TEST NO.	N_L**	ΔX (in.)	T_c ($^\circ$F)	T_h ($^\circ$F)	h_{eff} (Btu/hr-ft$^\circ$F)	Pressure (Torr)
1.1	2-1	5/16	-317	69	8.93×10^{-4}	5×10^{-5}
1.2	2-1	5/16	72	280	3.92×10^{-3}	1×10^{-5}
2.1	3-2	5/16	-303	73	2.84×10^{-4}	1.2×10^{-5}
2.2	3-2	5/16	73	293	2.8×10^{-3}	5.7×10^{-6}
3.1	4-3	5/16	-312	76	3.02×10^{-4} D	3.0×10^{-6}
3.1 (1R)*	4-3	5/16	-315	69	2.43×10^{-4}	2.0×10^{-6}
3.2	4-3	5/16	73	297	2.5×10^{-3}	1×10^{-5}
4.1	5-4	5/16	-315	77	3.12×10^{-4} D	1.6×10^{-5}
4.1 (1R)*	5-4	5/16	-319	73	1.49×10^{-4}	2.0×10^{-6}
4.2	5-4	5/16	71	295	2.56×10^{-3}	1×10^{-5}
5.1	6-5	5/16	-323	74	3.11×10^{-4} D	1.4×10^{-6}
5.1 (1R)*	6-5	5/16	-315	74	1.68×10^{-4}	1.8×10^{-6}
5.1 (2R)*	6-5	5/16	-319	67	2.00×10^{-4}	1.6×10^{-6}
5.2	6-5	5/16	67	297	2.00×10^{-3}	1.6×10^{-6}
6.1	7-6	5/16	-314	70	2.52×10^{-4}	1.0×10^{-6}
6.2	7-6	5/16	66	297	1.58×10^{-3}	7.0×10^{-6}
7.1	8-7	5/16	-313	69	2.79×10^{-4}	1.3×10^{-6}
7.2	8-7	5/16	71	298	2.24×10^{-3}	6.2×10^{-6}
8.1	9-8	5/16	-317	75	3.15×10^{-4}	2.3×10^{-6}
8.2	9-8	5/16	67	300	1.79×10^{-3}	1.5×10^{-6}
5.1 (3R)*	6-5	5/16	-317	74	2.00×10^{-4}	1.2×10^{-6}
5.2 (2R)*	6-5	5/16	72	302	1.90×10^{-3}	2.6×10^{-5}
5.1 (4R)*	6-5	5/16	-320	73	2.35×10^{-4}	8.0×10^{-7}
9.1 ±	0-0	4/16	-324	77	1.28×10^{-3}	3.0×10^{-6}
9.2 ±	0-0	4/16	72	301	4.81×10^{-3}	2.0×10^{-5}

* Repeat tests
** No. of layers of Al Mylar – No. of layers of nonwoven Dacron
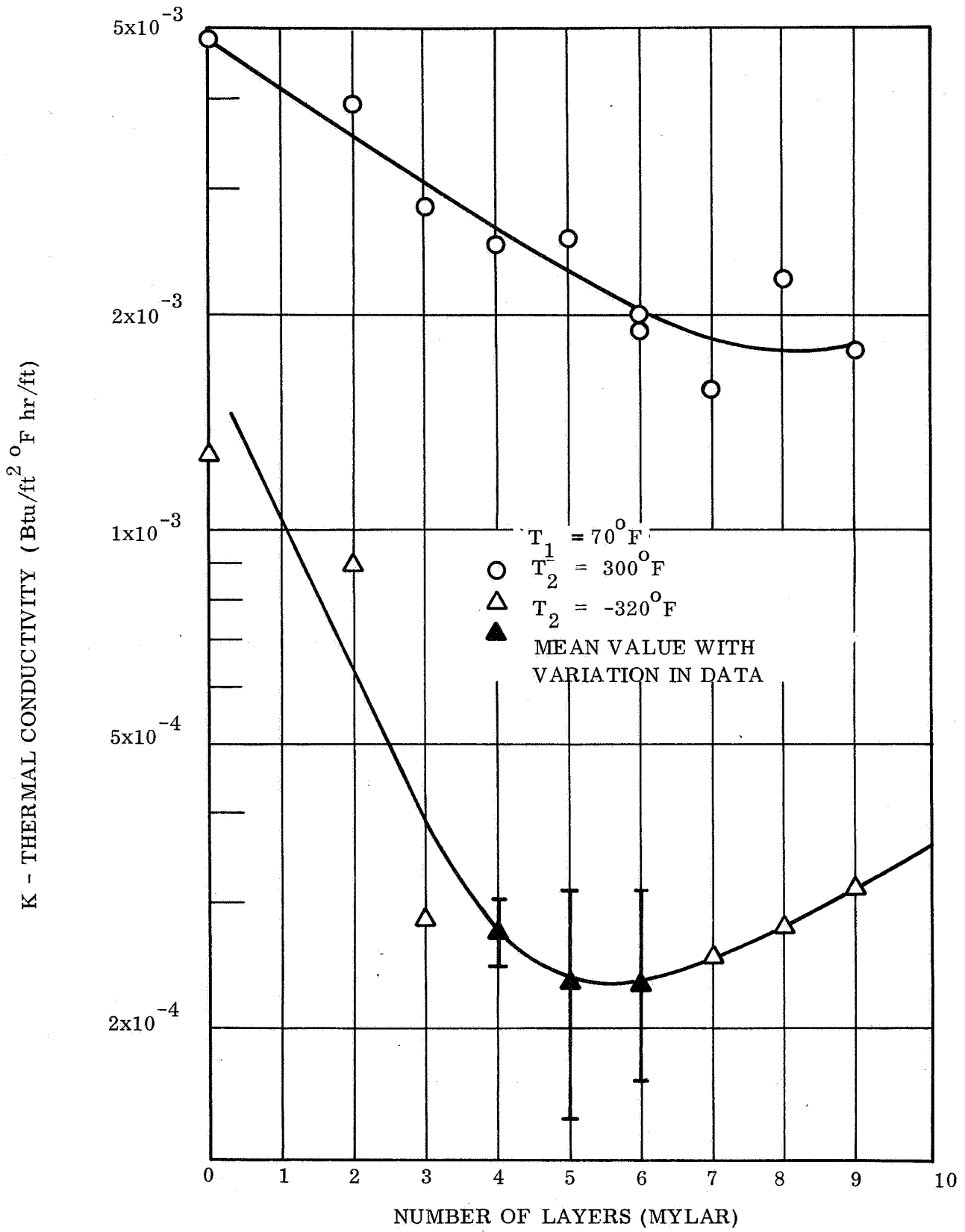± Felt samples
D Doubtful test point
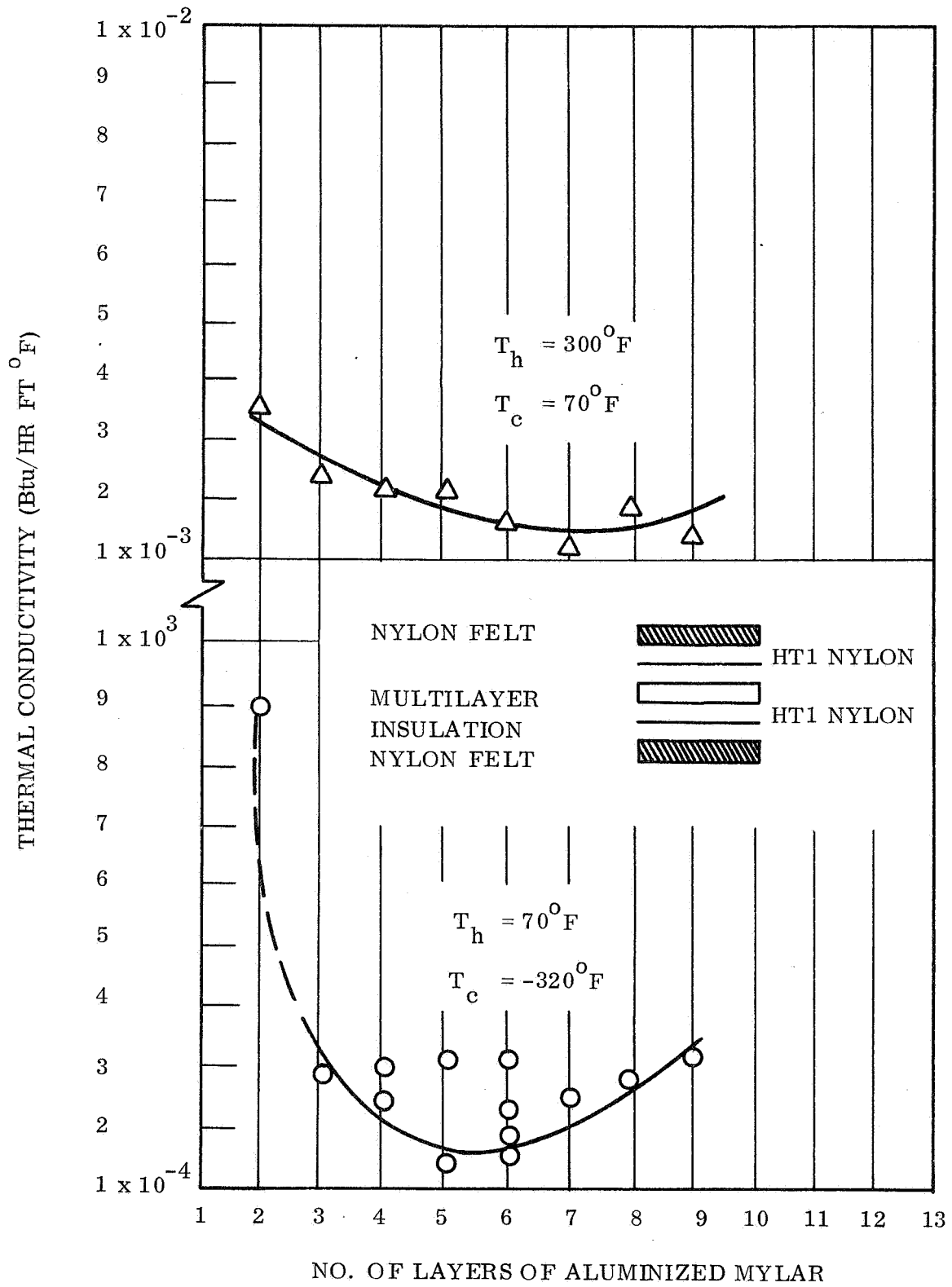
Figure 2-3. Variation in Conductivity with No. of Layers

Figure 2-4. Variation in Conductivity with No. of Layers (Weighted)

It was then assumed that the aluminized polyester film – nonwoven Dacron assembly was thermally in series with the nylon felt. Hence, having measured the effective thermal conductivity of the felt, the effective thermal conductivity of the balance of the layup was determined by using the relation:

$$K_{ML} = \frac{\Delta X_{ML}}{\dfrac{\Delta X_{TOT}}{K_{TOT}} - \dfrac{\Delta X_F}{K_F}}$$

where:

K = Thermal conductivity

ΔX = Thickness

Subscripts

ML = Multilayer

TOT = Total

F = Felt

It was also assumed that:

$$\Delta X_{ML} = \Delta X_T - \Delta X_F$$

Table 2-2 is a tabulation of the Task I results and Figure 2-5 shows the data graphically. The results are essentially unchanged, indicating an optimum at 5-6 layers for the cold case and 7-8 layers for the hot case.

Tests 5.1 (3R), 5.2 (2R), and 5.1 (4R) were run to assess the effect of temperature cycling on the effective thermal conductivity of multilayer insulation. It was felt that temperature cycling of the insulation sample while under pressure could have the effect of ironing out wrinkles in the aluminized mylar. This would in effect result in greater contact area

Table 2-2. Effective Thermal Conductivity of Multilayer Insulation Without Nylon Felt

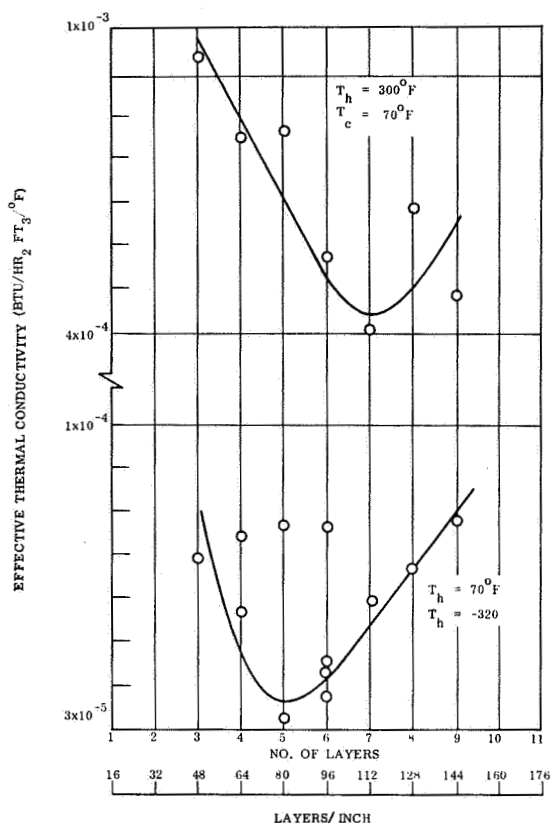| Test No.	k_{eff} (Btu/hr ft °F)
1.1	4.04×10^{-4}
1.2	2.25×10^{-3}
2.1	6.91×10^{-5}
2.2	1.06×10^{-3}
3.1	7.45×10^{-5}
3.1 (1R)	5.73×10^{-5}
3.2	8.74×10^{-4}
4.1	7.76×10^{-5}
4.1 (1R)	3.29×10^{-5}
4.2	8.92×10^{-4}
5.1	7.72×10^{-5}
5.1 (1R)	3.75×10^{-5}
5.1 (2R)	4.57×10^{-5}
5.2	5.99×10^{-4}
6.1	6.0×10^{-5}
6.2	4.29×10^{-4}
7.1	6.77×10^{-5}
7.2	7.15×10^{-4}
8.1	7.84×10^{-5}
8.2	5.10×10^{-4}
5.1 (3R)	4.57×10^{-5}
5.2 (2R)	4.32×10^{-5}
5.1 (4R)	5.51×10^{-5}

Figure 2-5. Effective Thermal Conductivity of Aluminized Mylar with **Nonwoven** Dacron Spacers (Without Felt)

between adjacent areas and, hence, result in a higher effective thermal conductivity. In order to verify the possibility of this occurring, three tests, were performed: a cold case test, a hot case test, and then a repeat of the cold case test. The results indicate a 17 percent increase in thermal conductivity, for no handling of the insulation. If the insulation is handled, and in doing so, fluffed or crinkled, the thermal conductivity should be less, as evidenced by tests 5.1 (1R) and 5.1 (2R). This problem of aluminized polyester film crinkling is discussed in more detail in Section 4.

It is also of interest to note that tests 5.1 (3R), 5.2 (2R) and 5.1 (4R) were performed after a newly-built-and-instrumented heater plate was installed, yet the results of tests 5.1 (1R, 2R, 3R, 4R) indicate reasonably good reproducibility.

The explanation for the existence of an optimum insulation density has already been discussed (Reference 1). References 5 and 6 provide data substantiating the existence of this minimum in the area of 50-70 layers/inch. There is no completely conclusive evidence that the effective thermal conductivity of these types of material are independent of thickness for a constant bulk density.

The data generated in this program show the hot temperature case optimum number of layers per inch to be higher than that for the low temperature case. This is consistent with what is expected theoretically. The following derivation follows that suggested by Reference 4 to show approximately the effect of temperature on the optimum number of layers of insulation.

If we neglect any gaseous conduction within the insulation then the heat transfer through the insulation consists solely of radiation and solid conduction. For n-1 reflective shields the radiant heat transfer can be written, approximately, as:

$$q_r \cong \frac{F \sigma (T_h^4 - T_c^4)}{n} \approx \frac{F \sigma \overline{T}^4}{n}$$

where:

F = net interchange factor

T = hot side temperature, cold side temperature

$\overline{T}$ = weighted average temperature

n = number of reflective shields

The solid conduction can be expressed approximately as:

$$q_c = cn (T_n - T_c) \cong cn \overline{T}$$

where

c = constant

2-10

The total heat transfer is:

$$q_t = cn\overline{T} + \frac{\mathcal{F}\sigma\overline{T}^4}{n}$$

The condition for a minimum total heat transfer is simply:

$$\frac{\partial q_t}{\partial n} = 0 = c\overline{T} - \frac{\mathcal{F}\sigma\overline{T}^4}{n^2} \text{ ,and } n_{min} = \sqrt{\frac{\mathcal{F}\sigma\overline{T}^3}{c}}$$

The ratio of the optimum number of layers at two different temperature levels is:

$$\frac{(n_{min})_{T_1}}{(n_{min})_{T_2}} = \sqrt{\left(\frac{\overline{T}_1}{\overline{T}_2}\right)^3}$$

The significance of the above equation is that as the mean temperature increases so does the number of layers of insulation required for minimum heat transfer rate.

It is important to note that the optimum insulation density listed in the literature as 50-70 layers per inch probably applies to cryogenic type insulation within the appropriate low temperature regime. Thus, for use in the temperature range of interest here, if the above relations hold, the ratio of $(n/n)_{min}$ may be as high as 1-1/2, and the higher temperature optimum could be 60 x 1-1/2, which is approximately the observed value.

2.2 TASK 2

2.2.1 TASK 2 DISCUSSION

This phase of the program was concerned with obtaining thermal conductance data on actual space suit material assembly samples as a function of compression for several temperature boundary conditions. Table 2-3 shows the constituent materials of the Configuration A, B and C layups. Each of these will be discussed separately. It should be noted that the same test sample was used in all of Configuration A tests, and that one test sample was used in Configurations B anc C test, except that parts of the insulation spacers were changed for Configuration C. Thus, the effect observed during Task 1 of flattening the

Table 2-3. Samples Tested in Task 2

Configuration	Constituent Materials
A	2 layers - rubberized cloth, dark gray, cloth facing body. 5 layers - 1/4 mil Mylar crinkled, aluminized one side, each layer followed by nonwoven Dacron. 2 layers - 1/4 mil Mylar crinkled, aluminized one side, followed by nylon marquisette. 1 layer - HT-1 nylon cloth
B	1 layer - rubberized cloth, dark gray, rubber facing body 1 layer - 6 oz nylon fabric, blue 2 layers - bladder cloth, light gray, (neoprene), cloth toward body 7 layers - 1/2 mil crinkled Kapton, aluminized both sides. 6 layers - separated by beta glass cloth 2 layers - beta glass cloth, heavy, white
C	Same as Configuration B except: 1 layer - neoprene bladder cloth, light gray replaces heavier dark gray rubber cloth 6 layers - beta glass marquisette, replace cloth in separators.

crinkled insulation may easily have occurred. In order to minimize such effects, we tested the fluffy layup conditions first, and increased the sample compression with each succeeding test. Another possible problem area affecting the results is due to the "curling" of the rubberized cloth. After testing had started, it was noted that the rubberized cloth could not be laid flat. Initially, only the edges curled, but later the entire 14 x 14 inch sample rolled itself into a small diameter cylinder, when samples were turned around. This could have affected the thermal conductance data at low compression (large spacing) adversely, since the tendency to curl exhibited by the rubberized material could result in a compression effect on the multilayer insulation.

Table 2-4 shows the Task 2 test results and related data. It should be noted that the Configuration A tests were not as extensive as were those for the fire-resistant Configurations B and C, since the A tests were halted upon receipt of Configuration B test samples.

2.2.2 TASK 2 RESULTS

2.2.2.1 Configuration A Results

A total of 6 test points at a 4/32 inch thickness of the sample were obtained. This thickness was such as to provide a minimum of compression, with the sample outside layers just barely in contact with the hot and cold plates. Several of these test points were repeat points, to check reproducibility.

Figure 2-6 shows some of the results graphically and provides comparison with other tests, in particular the comparison with test 14 of Reference 1 (the preceding contract period of this program). The current data shows lower conductivity values, which may be due to: (1) use of nylon marquisettes, spacers, and (2) better crinkling, since this was a new test sample. Data points for Configuration B are also shown. Although a plot of thermal conductance vs density (or thickness) may be more meaningful, the use of average temperature on the abscissa was mandatory as a comparative basis, since only one thickness was tested.

Of further interest is the reproducibility of data. The conductance of run A-3 and A-3A (the repeat run) are within 10 percent of each other. Similarly, run A-5 is a repeat of run A-1

Table 2-4. Task 2 Test Data Summary

| Task	Config.	Run	Compressed Thickness X (In.)	X' (Ft)	Thermal Conductivity K (Btu/Hr-Ft²°F/Ft)	Thermal Conductance K/ΔX (Btu/Hr-Ft²-°F)	Avg (°R)	Hot (°R)	Cold (°R)	Chamber Pressure (mm Hg)	Electric Power Input (Watts)	dT/dt	ΔT	Run Time Total/Data (Hours)	Comments
2	A	1	4/32	0.0104	3.03×10^{-5}	2.91×10^{-3}	333.6	530.1	137.0	2.0×10^{-6}	0.3067	0.0	3.0	18/2	Drift in Digital Voltmeter
2	A	2	4/32	0.0104	8.24×10^{-5}	7.92×10^{-3}	439.5	530.8	348.2	1.0×10^{-6}	0.3624	10.0	0.0	96/2	Drift in Digital Voltmeter
2	A	3	4/32	0.0104	1.25×10^{-4}	1.20×10^{-2}	581.8	634.0	529.5	2.4×10^{-6}	0.3289	0.0	5.2	120/3	Began K-3 Meas.
2	A	3A	4/32	0.0104	1.13×10^{-4}	1.08×10^{-2}	584.9	637.0	532.8	2.6×10^{-6}	0.3213	0.8	0.3	48/2	Repeat of Run 3
2	A	4	4/32	0.0104	1.93×10^{-4}	1.85×10^{-2}	639.0	744.5	533.5	2.8×10^{-6}	1.3267	5.3	15.0	120/2	Guard Heater Difficulty
2	A	5	4/32	0.0104	2.90×10^{-5}	2.78×10^{-2}	334.4	528.7	140.0	5.0×10^{-6}	0.2872	0.0	0.4	7/4	Repeat of Run 1
2	B	6	6/32	0.0156	4.54×10^{-5}	2.91×10^{-3}	334.0	529.9	138.0	1.0×10^{-7}	0.3030	0.0	1.5	7/4	Drift in Digital Voltmeter
2	B	7	6/32	0.0156	7.48×10^{-5}	4.80×10^{-3}	443.6	527.3	359.9	9.0×10^{-7}	0.2443	8.5	0.0	28/4	
2	B	8	6/32	0.0156	1.65×10^{-4}	1.06×10^{-2}	581.1	632.5	529.6	5.0×10^{-6}	0.2887	4.0	0.4	67/7	
2	B	9	6/32	0.0156	1.96×10^{-4}	1.26×10^{-2}	636.6	743.5	529.6	2.0×10^{-6}	0.7599	3.0	0.5	22/5	
2	B	10	5/32	0.0130	1.43×10^{-4}	1.10×10^{-2}	583.1	636.1	530.1	2.0×10^{-6}	0.3410	4.0	2.0	48/3	
2	B	11	5/32	0.0130	1.68×10^{-4}	1.29×10^{-2}	636.2	745.4	531.0	2.0×10^{-6}	0.7728	0.0	0.9	12/7	
2	B	13	5/32	0.0130	3.87×10^{-5}	2.98×10^{-3}	335.3	530.5	140.0	1.0×10^{-7}	0.3346	1.3	5.6	7/3	
2	B	14	5/32	0.0130	6.60×10^{-5}	5.07×10^{-3}	445.0	532.6	357.3	4.0×10^{-7}	0.2734	7.0	4.0	8/5	
2	B	15	4/32	0.0104	6.81×10^{-5}	6.54×10^{-3}	445.1	531.4	358.8	8.0×10^{-7}	0.3346	4.0	3.0	8/5	
2	B	16	4/32	0.0104	4.54×10^{-5}	4.36×10^{-3}	333.2	529.8	136.5	1.2×10^{-7}	0.4780	2.0	1.5	10/4	
2	B	17	4/32	0.0104	1.48×10^{-4}	1.42×10^{-2}	584.4	635.4	533.3	2.0×10^{-6}	0.3976				Sample Turned in Error
2	B	18	4/32	0.0104	1.58×10^{-4}	1.52×10^{-2}	638.8	747.2	530.3	5.0×10^{-6}	0.9058	Data Invalid			Power Failure and Contamin.
2	B	19	4/32	0.0104	1.14×10^{-4}	1.10×10^{-2}	586.5	643.4	529.5	6.0×10^{-7}	0.3338				Power Failure and Contamin.
2	C	20	6/32	0.0156	3.02×10^{-4}	1.93×10^{-2}	568.6	604.4	532.8	2.0×10^{-6}	0.3784	0.0	2.3	74/N.A.	
2	C	21	6/32	0.0156	1.81×10^{-4}	1.16×10^{-2}	639.1	746.6	531.5	3.0×10^{-6}	0.6937	0.0	0.8	12/23	
2	C	22	6/32	0.0156	1.52×10^{-4}	9.75×10^{-3}	589.2	688.6	529.8	2.7×10^{-6}	0.2867	0.0	1.7	26/2	
2	C	23	6/32	0.0156	7.19×10^{-5}	4.60×10^{-3}	445.8	528.6	363.0	2.5×10^{-6}	0.2188	6.7	2.8	31/2.7	
2	C	24	6/32	0.0156	4.39×10^{-5}	2.81×10^{-3}	333.2	530.3	136.0	1.4×10^{-7}	0.2971	0.0	2.9	28/3.5	
2	C	25	5/32	0.0130	3.48×10^{-5}	2.68×10^{-3}	332.2	524.4	140.0	2.0×10^{-7}	0.2921	2.2	0.6	26/2.5	
2	C	26	5/32	0.0130	1.72×10^{-4}	1.32×10^{-2}	632.5	736.8	534.2	1.8×10^{-6}	0.7436	0.3	0.8	25/3	
2	C	27	4/32	0.0104	2.54×10^{-4}	2.44×10^{-2}	637.4	742.3	532.5	3.2×10^{-6}	1.4110	0.0	0.1	8/2.5	
2	C	28	4/32	0.0104	4.15×10^{-5}	3.98×10^{-3}	337.5	537.0	138.0	5.0×10^{-8}	0.4402	0.0	0.4	7.5/3.5	
2	C	29	3/32	0.0078	3.35×10^{-4}	4.30×10^{-2}	334.5	529.9	139.0	3.0×10^{-8}	4.5874	1.1	0.0	26/3	
2	C	30	7/64	0.0091	8.82×10^{-5}	9.70×10^{-3}	335.0	529.9	140.0	5.0×10^{-7}	1.0032	3.4	0.2	13/6	
2	C	31	7/64	0.0091	4.85×10^{-4}	5.33×10^{-2}	635.8	739.4	532.1	2.0×10^{-6}	3.0789	1.1	0.0	6.5/3.5	
2	B	12	5/32	0.0130	2.33×10^{-2}	1.79	568.2	602.5	533.9	(5.00 psia nitrogen)	33.646	0.8	0.3	3.1/1.0	Rapid Approach to Equilib.
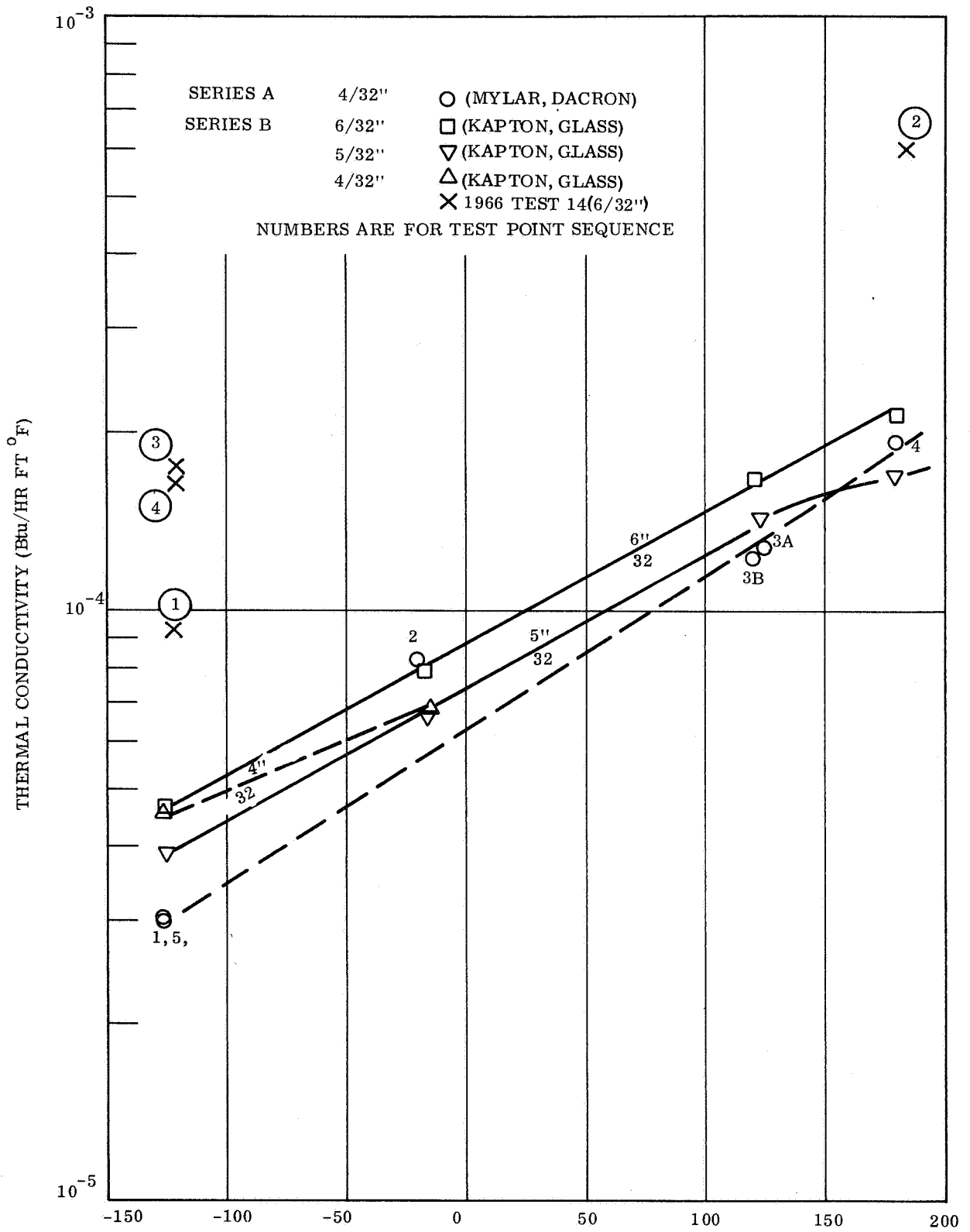
Figure 2-6. Thermal Insulation Conductivity Vs Average Temperature
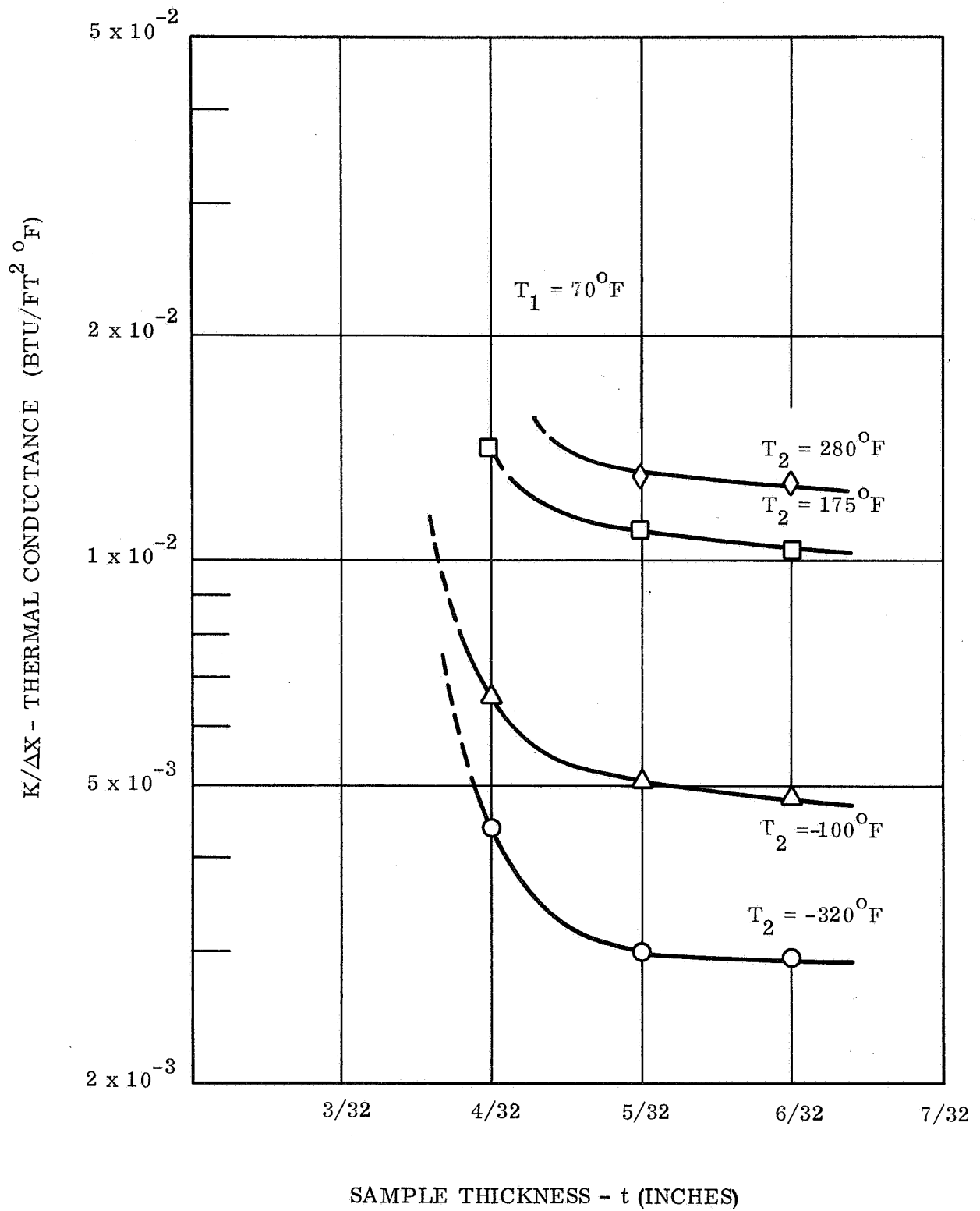
Figure 2-7. Configuration B Insulation: Effective Conductance

The points B-18 and 19 were taken after a regional power failure, which resulted in diffusion pump oil backstreaming, which contaminated the sample edges. This, however, was not discovered until after the tests, since the vacuum system had been blanked-off within a few minutes after power failed and it had been assumed that there was no damage. These data points are, therefore, assumed to be invalid.

2.2.2.3 Configuration C Results

This group of 12 tests presents the largest and, perhaps, the most reliable group of experimental data. It should be noted that the test samples used in this group of tests are the same as those used for Configuration B, but for the following exceptions:

a. the diffusion pump oil contaminated outer layers of beta glass cloth were replaced

b. neoprene bladder cloth (grey) replaced the curling, heavier, dark grey rubberized cloth

c. beta glass marquisette replaced the beta glass cloth used for aluminized Kapton separation in Configuration B.

It may be of particular interest that an attempt was made to establish the trend of the effective thermal conductance vs density curve for high density, i.e., tight compression (or small sample thickness) conditions. Figure 2-8 shows the results of these tests. Since the general trend of the data had been demonstrated in the Configuration B tests, and time was scarce, detailed compression tests were performed at the extreme boundary temperature conditions of 280°F and -320°F only, with intermediate boundary temperature data obtained at the 6/32 inch thickness only. The results are both satisfying and interesting. As has been observed earlier, the increase in compression (or density) is accomplished by an increase in the solid conduction contribution. Below 4/32 inch sample thickness, the effective conductance increased almost linearly with thickness. This is to be expected on the basis of contact conductance results observed for solids, where the number of contact points increased nearly linearly with load, resulting in a proportionate increase in effective conductance. Conversely, it can be seen from Figure 2-8 that the thermal conductance approaches a constant value at spacings of 6/32 inch (low density) where most of the heat transfer is by radiation.
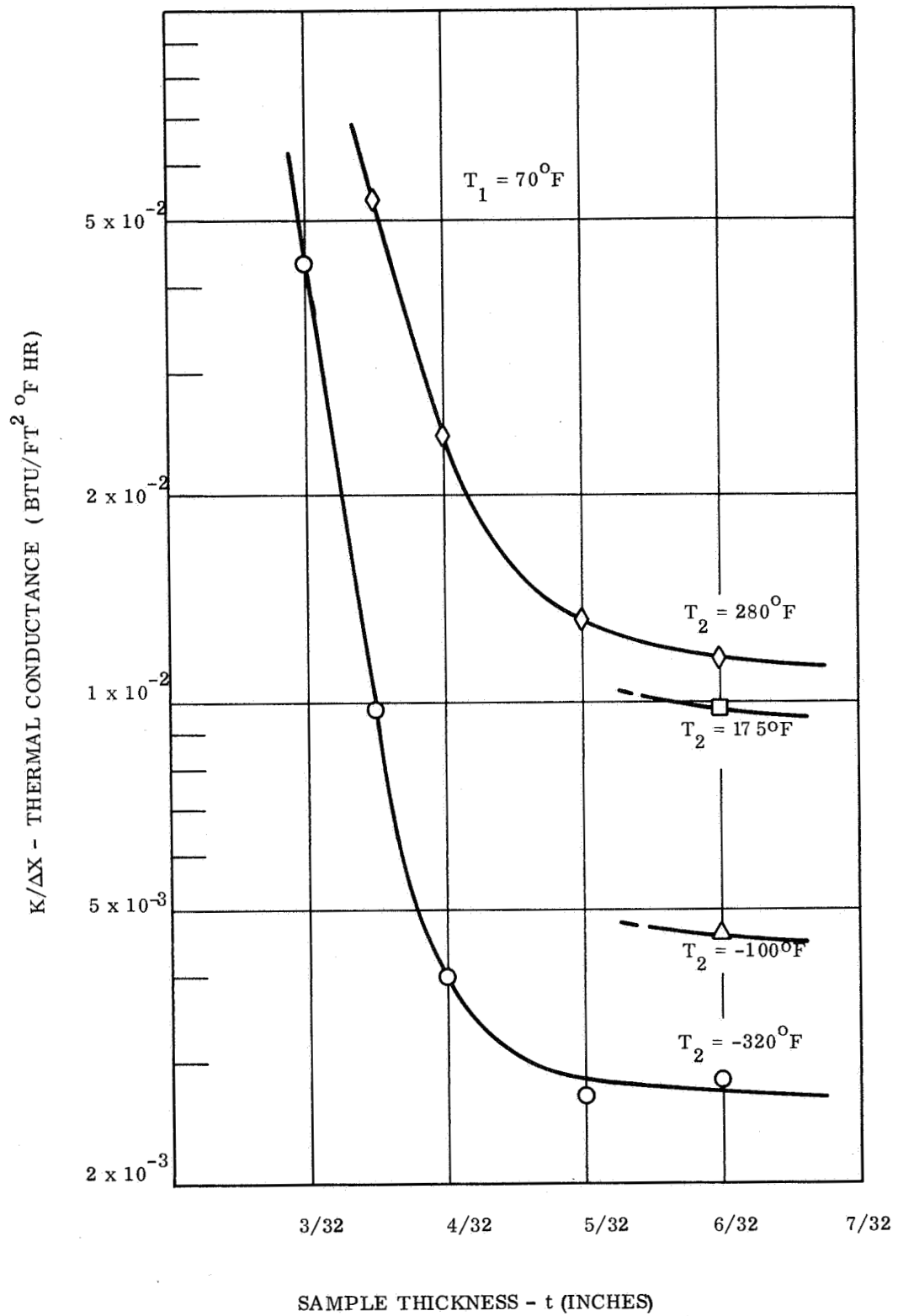
Figure 2-8. Series C Insulation: Effective Thermal Conductance Vs Thickness

2.2.2.4 Summary of Task 2 Results

One question of interest was that of determining which types of metallized film and spacers would prove the best and most reproducible or predictable spacesuit thermal insulation. For this purpose plots of the data from Configurations A, B, and C are presented on one graph, shown in Figure 2-9. This graph indicates that the Configuration A insulation is slightly better than the others, but otherwise the results are remarkably similar over the range of thses tests and conditions.

Furthermore, as can be seen in Figure 2-6 this insulation shows much better thermal performance than is shown for that of Test Series 14 in References 1 and 3.

Can the thermal performance of this insulation be improved significantly by further work? The answer to this must be obtained by experimental work, rather than by analysis. However, a more fundamental question is whether further improvement is needed. It would seem that the tested insulations appear relatively adequate in the uncompressed state, but that thermal insulation performance for the compressed insulation needs to be improved. Furthermore, the resiliency and ability of the insulation to separate the layers where the compressive load is removed needs further work, to assure the predictability of spacesuit thermal performance as well as extended life reproducibility of such performance.
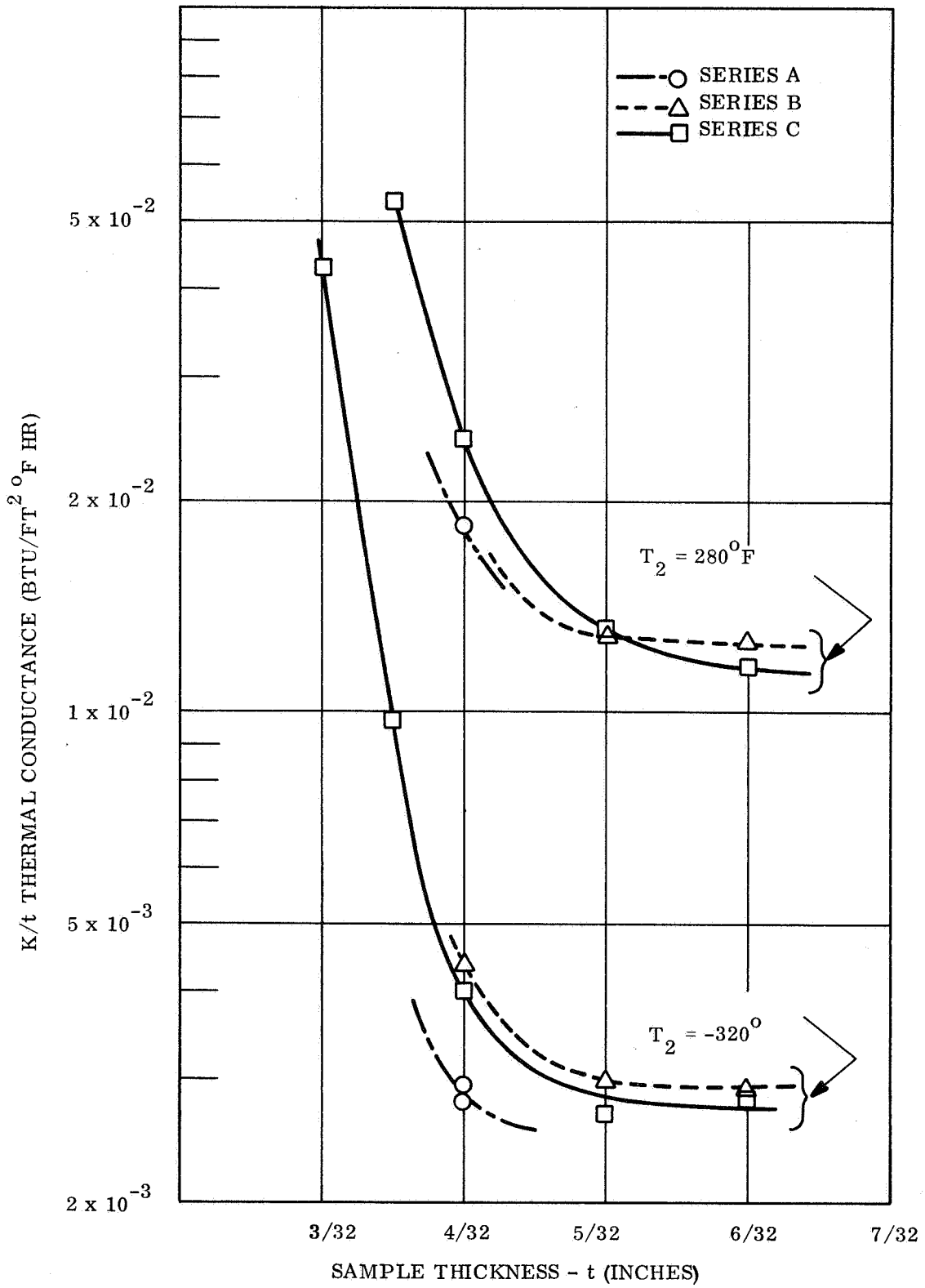
Figure 2-9. Insulation Sample Comparison: Thermal Conductance Vs Thickness

2.3 EFFECTS OF ENVIRONMENTAL PRESSURE

An item of significant interest in vacuum thermal insulation studies is the effect of gas pressure on the insulation thermal conductivity. In order to obtain such information, the Configuration B insulation was tested at 5 psia nitrogen in test B-12 for a thickness of 5/32 inch at $142.5^{\circ}F$ and $73.9^{\circ}F$ boundary conditions. The measured conductivity was 2.33×10^{-2} Btu/hr-ft-$^{\circ}F$. This compares with a value of 1.3×10^{-4} Btu/hr-ft-$^{\circ}F$, as interpolated from Figure 2-5, for vacuum conditions. It can be assumed from this that the gaseous conduction contribution contributes the difference, or nearly 2.32×10^{-2} Btu/hr-ft-$^{\circ}F$.

In order to check this, it was assumed that the effective thermal conductance at 5 psia (nitrogen or oxygen) can be predicted by adding the measured vacuum thermal conductance and the gaseous layer conductance and by assuming a gas layer equal in thickness to two-thirds the spacing. For this example we used a gas film of 0.10 inch and a thermal conductivity of 0.016 Btu/hr-ft-$^{\circ}F$. This gave a total conductance of 0.97 Btu/hr-ft-^{2}F for the gas film plus vacuum insulation, or slightly more than one half of the measured value of 1.79 Btu/hr-ft^{2}-$^{\circ}F$ for Test B-12. This implies that excessive heat losses existed during the test or that there is an added heat transfer mechanism which we have not considered. Since a test had been performed on double gold coated Kapton recently, this data, which was obtained on another test rig, was examined in a similar manner. The results were better, in that the measured value of conductance and that for a gas film equal to the void thickness were nearly equal. Figure 2-10 shows curves and data points for thermal conductivity of multilayer insulations vs. residual gas pressure from various sources. On the basis of this plot, the test point B-12 data looks reasonable. Only further testing can provide greater assurance for this type of data.
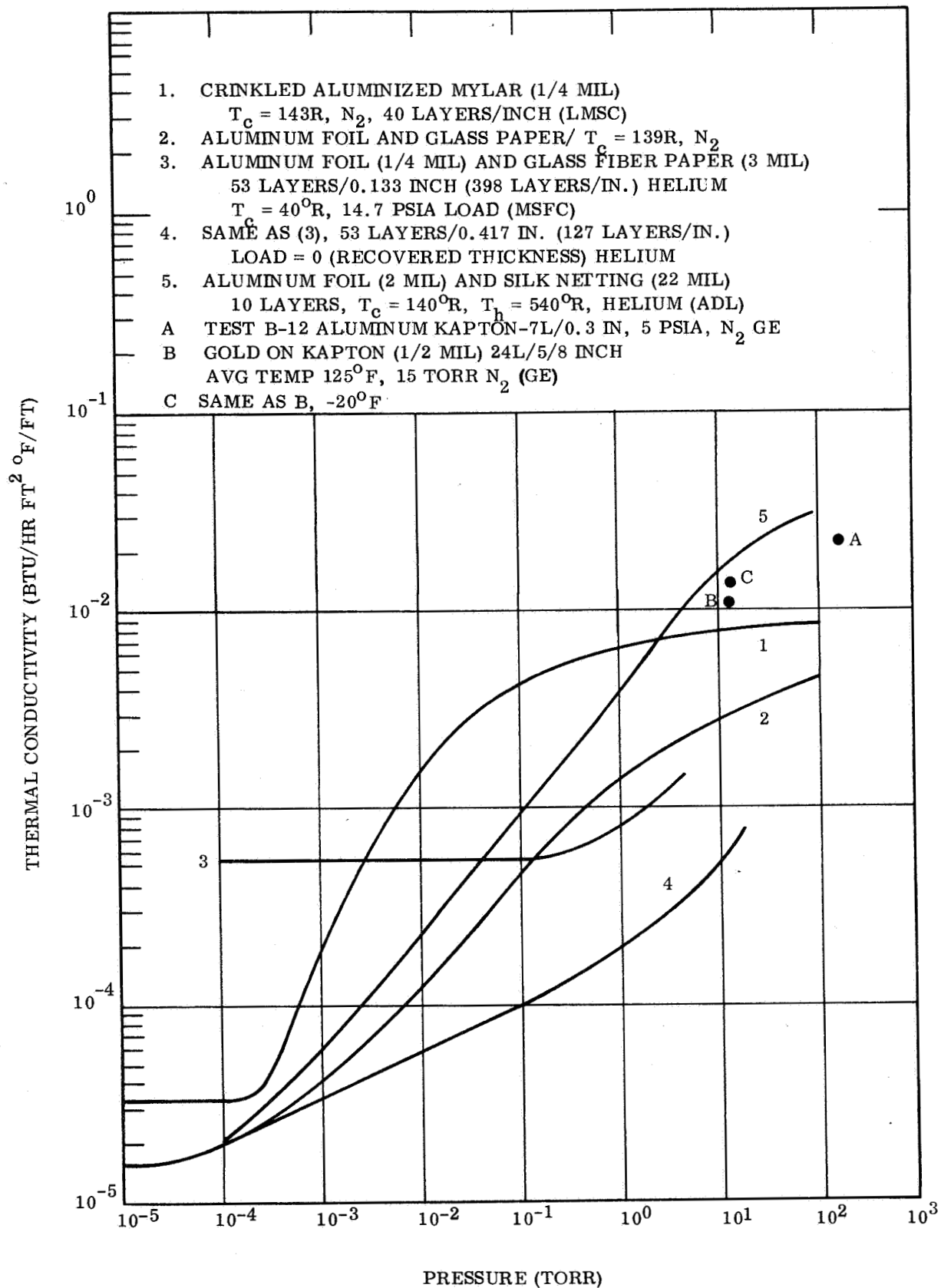
Figure 2-10. Thermal Conductivity vs Residual Gas Pressure

SECTION 3

TEST APPARATUS AND PROCEDURES

3.1 TEST APPARATUS

The experimental work described in this report was carried out using a guarded hot plate, twin sample test apparatus, designed specifically for the measurement of the thermal conductance of multilayer insulations. The construction of the apparatus generally follows the approach outlined in ASTM Standard C177-45. Although the apparatus is described in detail in Reference 1, several changes in equipment and procedures have been made, which makes it desirable to provide a description.

This apparatus consists of a flat heater plate and two cold plates. Two identical samples, 14 1/4 inches square, are tested simultaneously in the apparatus to provide an average value,to compensate in part for any sample inhomogeneity. A schematic view of this apparatus is shown in Figure 3-1, and a photograph of the apparatus is shown in Figure 3-2. The heater plate is made in two separate sections: (1) the main heater (actual test area), and (2) a guard heater. Each section is constructed of a mica heater sandwiched between two thick plates that form the top and bottom of the heater, providing a nearly isothermal surface.

The guard heater maintains an adiabatic boundary condition on the perimeter of the main heater. The cold plates are constructed of 3/8 inch thick copper plate, to which is soldered a 1/4 inch copper tube laid out in a serpentine fashion. Various fluids were circulated through the cold plate tubes to maintain a nearly isothermal surface at desired cold plate temperatures.

Both faces of the heater plate and cold plates were sprayed with a flat black lacquer to reduce the radiation resistance between the plates and the multilayer assemblies. A multilayer aluminized Mylar blanket was wrapped around the outer perimeter of the entire assembly, in order to help provide a more nearly adiabatic boundary condition (see Figure 3-8). The support structure was fabricated from Textolite, a poor thermal conductor, to reduce sources of error due to heat leaks.
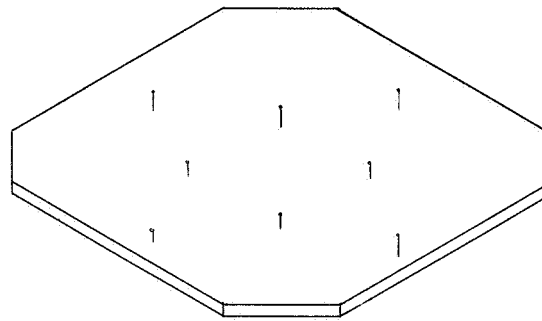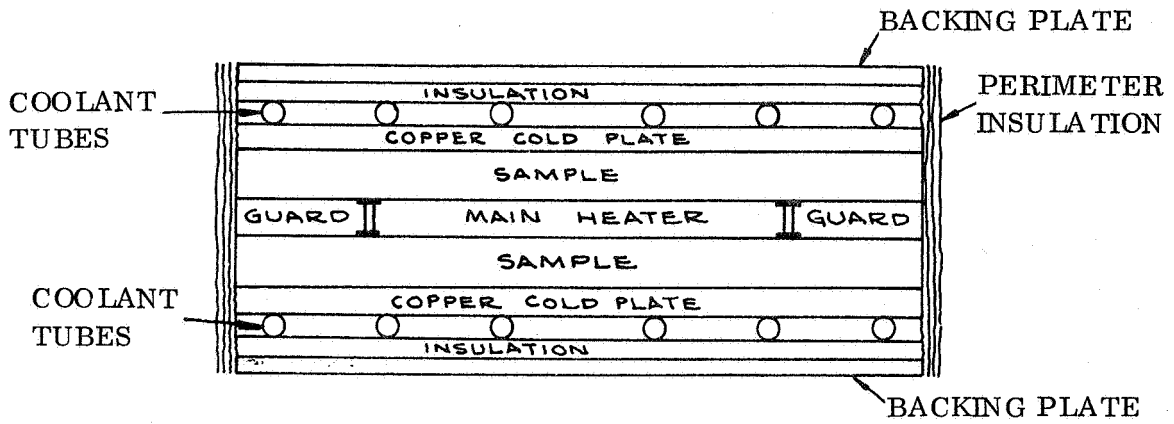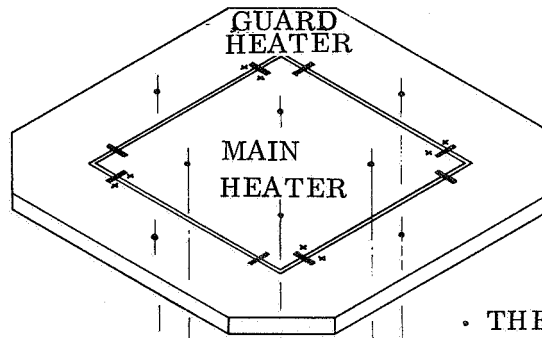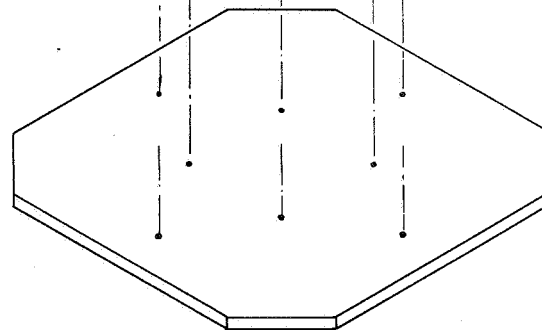
Figure 3-1. Schematic Diagram of Guarded Hot Plate Test Apparatus
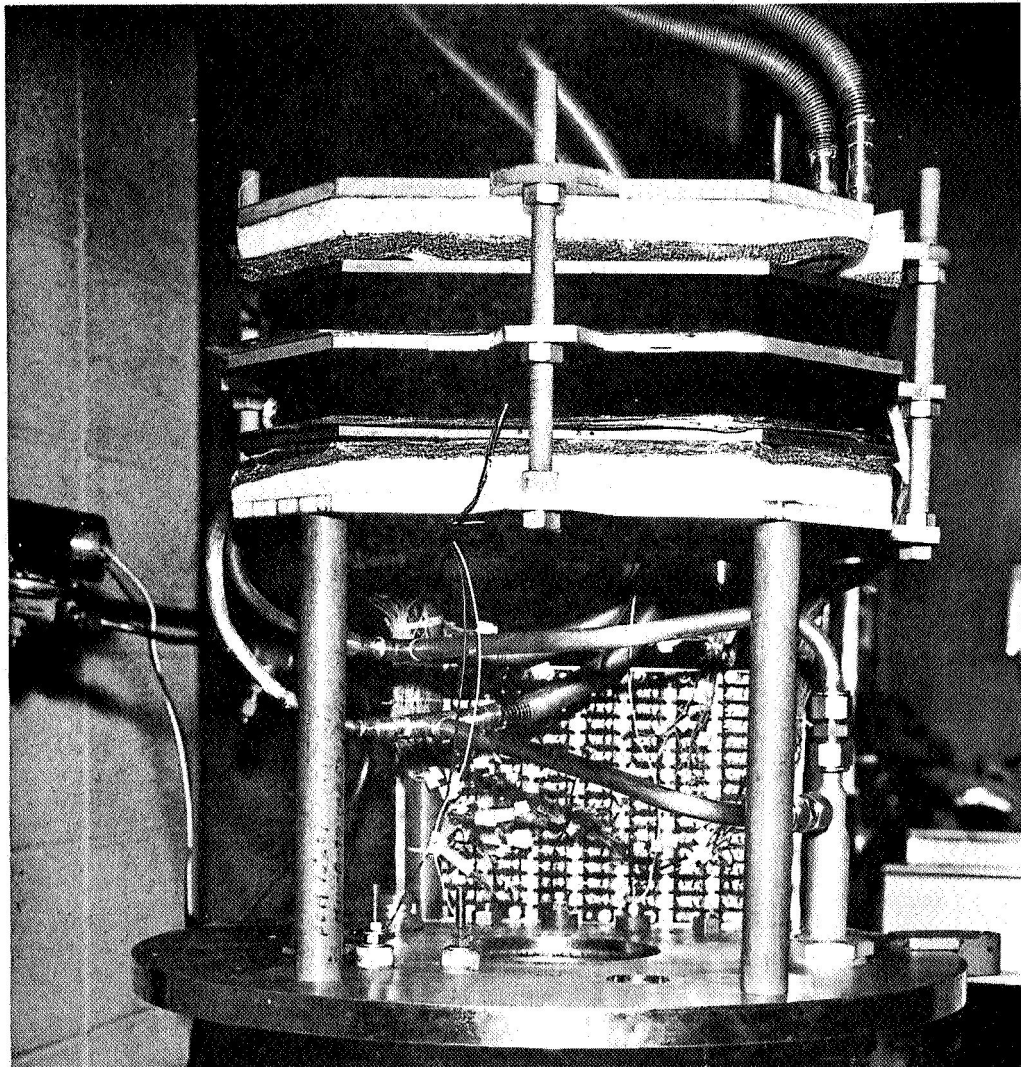
Figure 3-2. Guarded Hot Plate Test Apparatus

The heater plate, originally made of copper, was replaced by a thicker aluminum heater plate in September 1966, at the conclusion of Task 1, test 8.2. The reasons for this change were: (1) frequent electrical shorts between embedded thermocouples and heater circuit, and (2) undesirable warpage resulting in non-flatness of heater plate. The thicker aluminum plates maintained much better flatness characteristics under heat cycling and other loading conditions. The effects of the flatness deviation on the data are discussed elsewhere.

The center portion of the main heater plate has dimensions of 8.23 inches by 8.23 inches and is fabricated from heat treated aluminum alloy. (The plate used previously was copper.) Electric resistance heaters are embedded about 3/8 inch below the surface of the 3/4 inch plate; they have a total electrical resistance of about 17.95 ohms at 70°F. Four chromel-alumel thermocouples are embedded in each face about 0.16 inch deep at locations shown in Figure 3-2. The surrounding guard heater is fabricated in the same manner, and is connected to the main heater by 16 small, rigid plastic strips which also provide about 1/16 inch separation between heaters (Figure 3-3). The measured heat capacity of the main heater is 0.279 watt-hr/$^{\circ}$F (0.952 Btu/$^{\circ}$F), and the measured effective conductance between the main and guard heaters is 0.096 watt/$^{\circ}$F.

The cold plates were fabricated of copper and are the same size and plan form as the heater plates; copper tubing is brazed to the back surface for circulating thermal conditioning fluids. Eight chromel-alumel thermocouples are embedded in the face of each plate, as shown in Figure 3-2.

The electrical power inputs to the main and guard heaters were regulated by two 40-volt dc power supplies. The original test procedure, used in the initial phase (Task 1) of the program, provided a system in which the power supplies were activated and deactivated by temperature controls for the heater plates. The circuit for this is shown in Figure 3-4. This technique was discarded after that phase of the program in favor of a constant voltage input to the main heater, with a composite circuit of four different thermopile elements used to regulate the guard heater power (Figure 3-5).
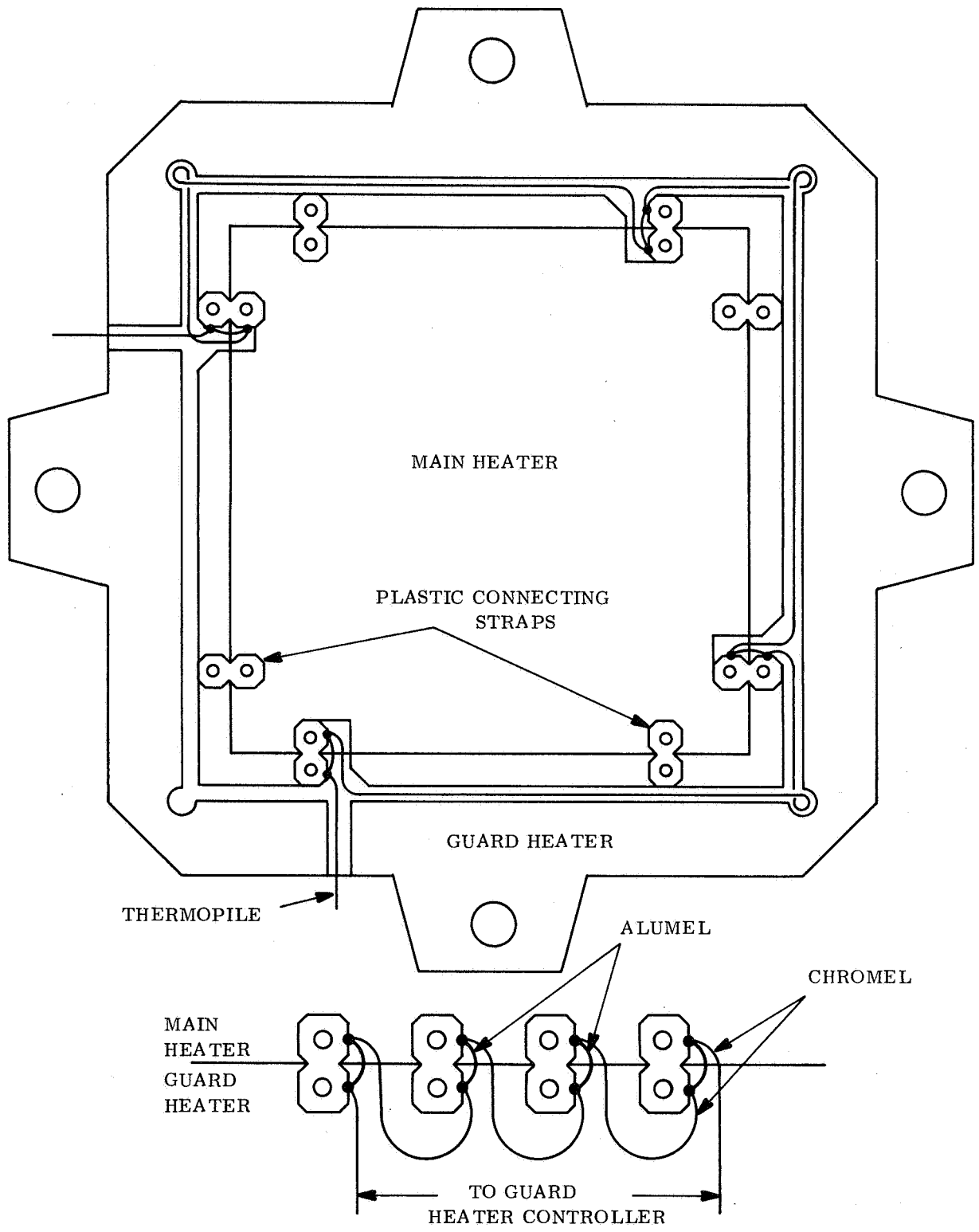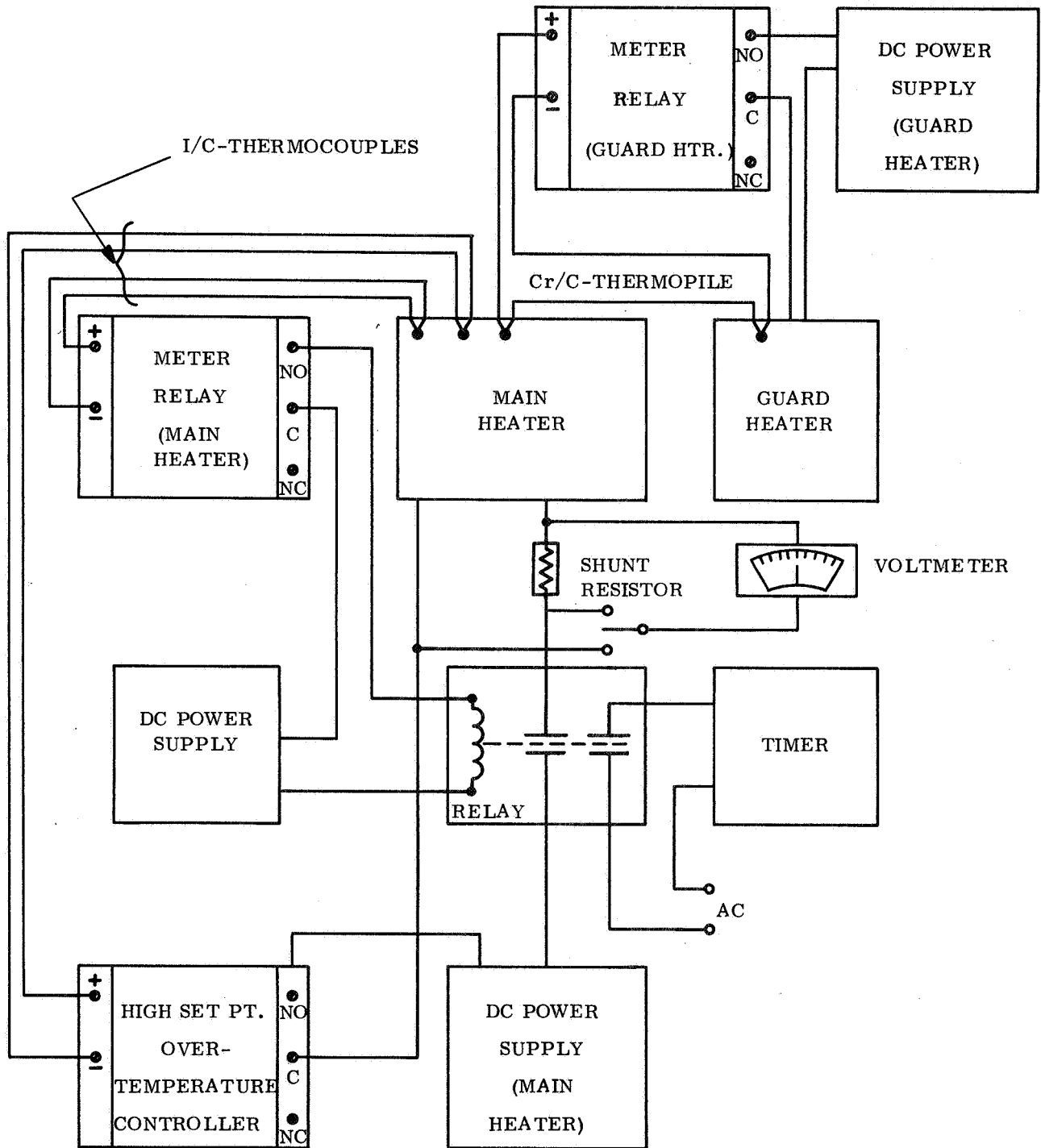
Figure 3-3. Heater Plate Thermopile Circuit

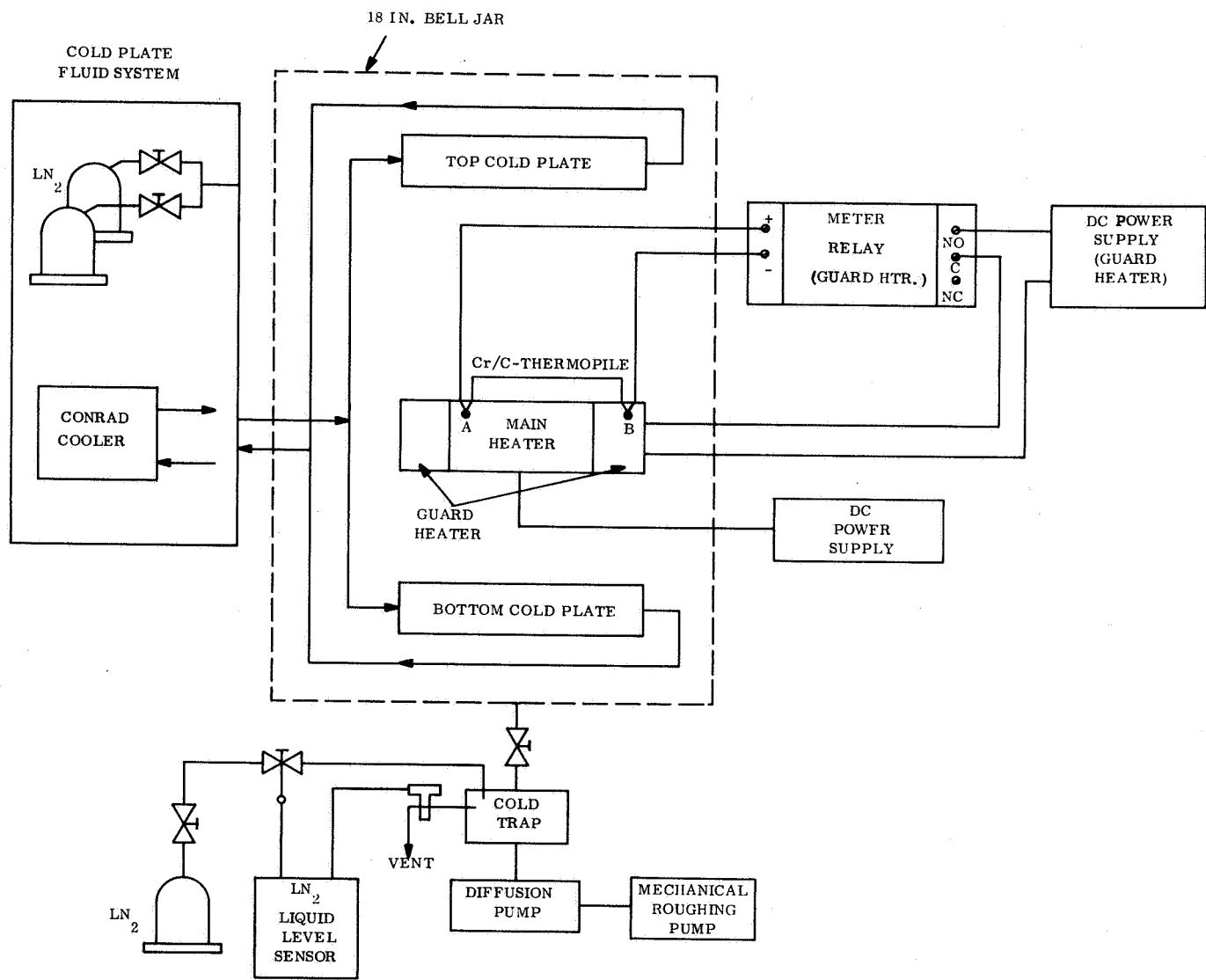Figure 3-4. Schematic of Instruments and Control -- Task 1

Figure 3-5. Schematic of Guarded Hot Plate Control System

Temperature controls were also used to maintain a nearly constant temperature in the cold plates and to provide an over-temperature cutoff for the main heater power. For cold plate temperatures below 0°F, liquid nitrogen and nitrogen "boil-off" gas were regulated by thermally actuated control valves to maintain the desired cold plate temperatures. For cold plate temperatures above 0°F, a Conrad heater-chiller unit, utilizing a silicone fluid, provided thermal conditioning for the cold plates.

In addition to the test apparatus, the experimental setup included an NRC Coater Vacuum System, two 40-volt regulated dc power supplies, and other equipment to regulate the thermal boundary conditions. The NRC Coater Vacuum Chamber is a diffusion vacuum system with pumping capability to provide pressures down to nearly 10^{-9} torr in an empty chamber. The system consists of an 18-inch diameter bell jar chamber, a 15 cfm mechanical pump, a 6-inch diffusion pump, a base plate with electrical feedthroughs, a cold trap, and various gauging and valving apparatus. The chamber pressure is measured with two thermocouple vacuum gauges and one hot filament ionization vacuum gauge with a range from 10^{-3} to 10^{-8} torr. A photograph of the vacuum system is shown in Figure 3-2.

3.2 INSTRUMENTATION

Adequate thermocouple instrumentation was provided to monitor temperature histories in both cold plates, the main heater plate, and the guard heater. All thermocouples were chromel-alumel and were referenced to a carefully controlled ice bath junction. The thermocouples were located in the plates to obtain representative distributions of temperature measurements and to indicate the degree of thermal equilibrium at any given time. All thermocouple temperature data were measured and recorded as voltage outputs, using the multirange digital voltmeter data system shown in Figure 3-6. Beginning with the Configuration A tests in Task 2, the main heater plate thermocouple outputs were also monitored and recorded, using a Leeds and Northrup K-3 potentiometer to obtain a more accurate evaluation of the power input corrections due to thermal transients.

Two sets of four chromel-alumel differential thermopile elements were installed between the main and guard heaters to sense the average temperature difference between the two heater plates. One set was connected to a controller which switched the guard heater on and off to maintain a minimum guard-to-main heater plate temperature difference. The second set was used to indicate and record the mean temperature difference on the digital voltmeter system. After the Task 2 Configuration B tests, the thermopile circuit output was switched to the K-3 precision potentiometer readout so that peak-to-peak thermopile variations rather than random variations could be evaluated.

The evaluation of power input to the main heater was made by measuring the voltage drop across the main heater, and by measuring the voltage drop across a 5-ohm shunt resistance in the line. Both voltages were measured and recorded using the digital voltmeter system. Line current was evaluated from the shunt voltage to determine the power dissipation in the heater.
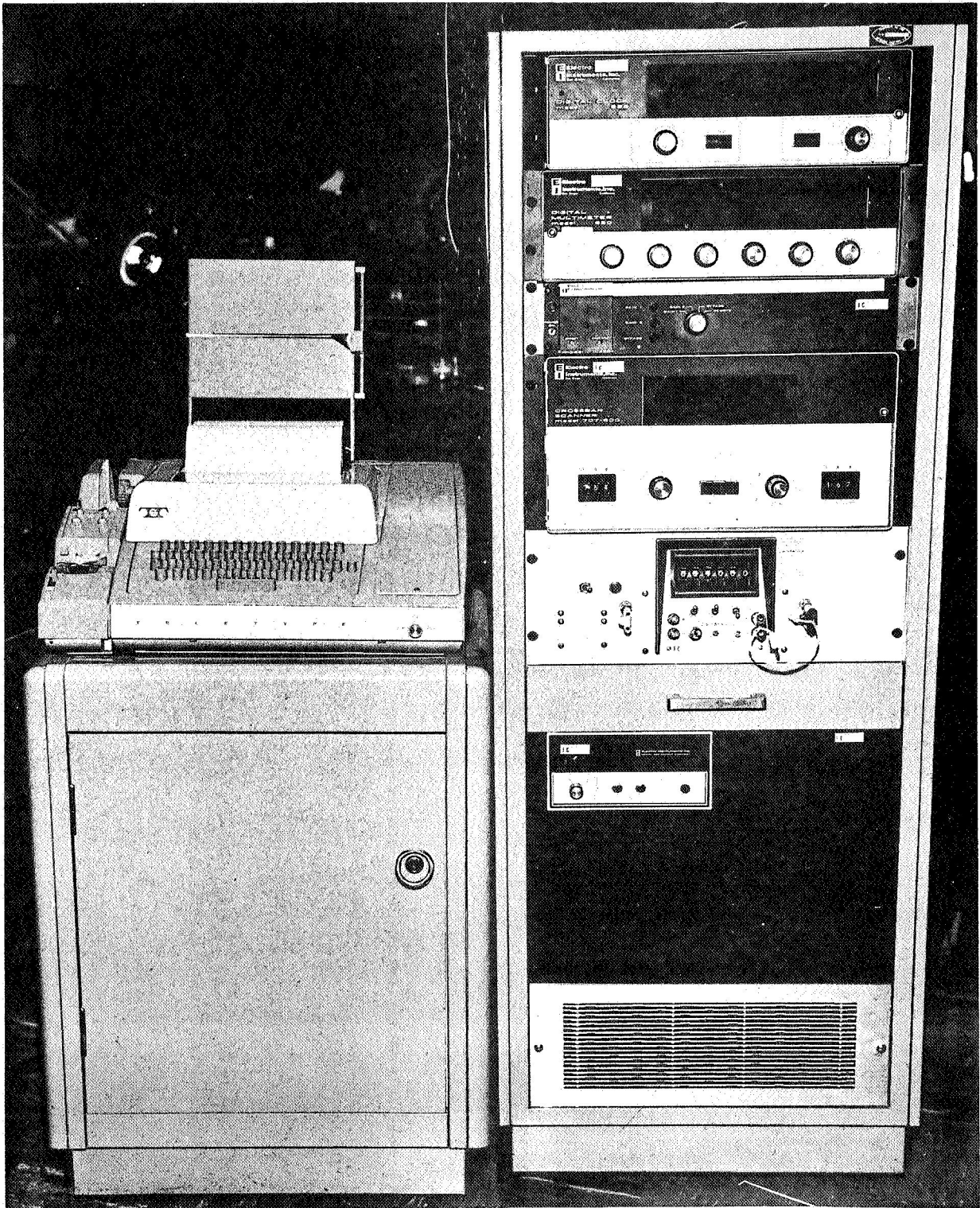
Figure 3-6. Electro Instruments Data System

3.3 TEST PROCEDURE

As stated previously, test procedures were updated continually throughout this program. For this reason the procedures used in Task 1 differed significantly from those of Task 2. In fact, there were minor changes in procedure during the work of Tasks 1 and 2. These procedures are described below.

3.3.1 TASK 1 TEST PROCEDURE

A typical test procedure is as follows:

a. The test sample is mounted in place and the sample thickness is set by measuring the plate spacing (top and bottom) at four different locations with a gauge block.

b. The bell jar is evacuated to a pressure of 10^{-4} torr, then backfilled with dry nitrogen and reevacuated to a pressure less than 10^{-4} torr. The purpose of this step is to purge the system for the majority of the entrapped water vapor prior to the introduction of any cryogenic fluid to the cold plates.

c. The main heater controller is energized, the set point is adjusted and the cold plate fluid is pumped through the cold plate.

d. When the main heater, guard heater and cold plates reach their respective set points, the main bell jar gate valve is closed and the bell jar is backfilled with dry N_2. The bell jar pressure is maintained between 50-100 mm Hg for 10-15 minutes and then reevacuated. The reason for this procedure is discussed in the following section.

e. The bell jar pressure is maintained at less than 10^{-5} torr for the balance of the test.

f. The main heater power supply is adjusted so that the power cycle is such that the power remains on for 80 to 90 percent of the time.

g. The system is allowed to remain in this state until an equilibrium state is achieved. Equilibrium is defined as the condition where the average power does not change more than $\approx 1\%/4$ hours.

A typical main heater plate power profile is shown in the following sketch:
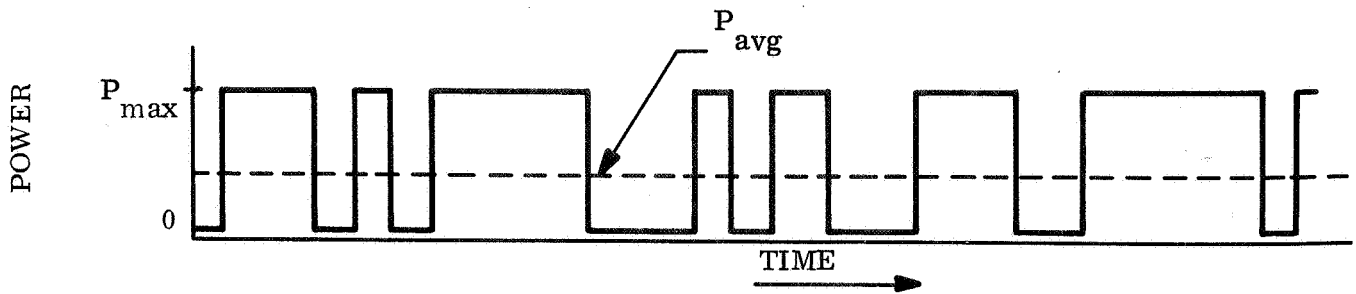
The effective thermal conductivity can be calculated as follows:

$$k_{eff} = \frac{E_h \cdot E_s \cdot t_t \cdot \Delta X}{R_s \cdot t_c \cdot A (T_h - T_c)}$$

where:

E_h = main heater voltage drop

E_s = shunt resistance voltage drop

A = total heat transfer area

R_s = shunt resistance

t_t = timer time

t_c = clock time (time between successive timer readings)

ΔX = sample thickness temperature difference between heater plate and cold plates

T_h, T_c = insulation boundary temperatures.

After several tests had been completed it was decided to modify the test procedure some-what. After the completion of step e in the previously outlined test procedure, the time average power was calculated and the main heater controller was overridden so as to allow providing the main heater with a constant power input equal to the previously estimated average value. Several adjustments in power were made in accordance with the relationship:

$$\frac{(E_h)^2 \, new}{R_h} = \frac{(E_h)^2 \, old}{R_h} - W \, C_p \, \frac{dT}{dt}$$

where: $W C_p$ =   heat capacity of main heater plate

$\dfrac{d\,\overline{T}}{d\,t}$ =   time rate of change of main heater temperature

R_h =   main heater resistance

Reference was made to the requirement of maintaining the bell jar pressure below 1×10^{-5} torr. In order to keep the conduction through the trapped gas within multilayer insulation to less than 10 percent of the radiation heat transfer term the pressure internal to the multi-layer insulation must be maintained less than 1×10^{-5} torr.

3.3.2 MEASUREMENT OF HEATER PLATE HEAT CAPACITY AND CONDUCTANCE

Two measurements were made on the test fixture to determine the main heater plate heat capacity and the conductance between the main heater and guard heater plates. These measurements are described in order.

The procedure followed in determining the main heater plate heat capacity was as follows:

a.   Place multilayer insulation sample in test fixture to act as insulation for main heater plate.

b.   Evacuate bell jar to a pressure less than 1×10^{-5} torr.

d.   Using the guard heater temperature controller to track the main heater plate temperature behavior, a step increase in main heater power was initiated.

d.   The main heater plate temperature behavior was recorded.

The main heater plate heat capacity can be determined from the following relationship:

$$W C_p = \frac{P}{d\overline{T}/dt}$$

The measured value was 0.954 Btu/$^\circ$F for the copper plate main heater.

The conductance between the main heater and guard heater has been determined in order to verify the accuracy of the guarded hot plate apparatus as a tool in the measurement of the thermal conductivity of multilayer insulations.

The main heater - guard heater conductance was measured in the following manner:

a.   Place multilayer insulation sample in test fixture to act as insulation for main heater plate.

b.   Evacuate bell jar to a pressure less than 1×10^{-5} torr.

c.   Disconnect the guard heater temperature controller. No power is supplied to the main heater.

d.   Apply a step change in power to the guard heater in order to raise the guard heater temperature by 10 to 15°F. Then remove all power.

e.   Record the main heater - guard heater temperature difference versus time.

Assuming that the outer edge of the heater plate is sufficiently well insulated to be considered an adiabatic surface, the following expression can be used to determine the guard - main heater conductance, h_g:

$$h_g = \frac{W \, C_p \, d\bar{T}/dt}{(T_{gh} - T_{mh})_{LMTD}}$$

where: $(T_{gh} - T_{mh})_{LMTD}$ = Log mean temperature difference between the main heater and guard heater over the test time span.

The measured conductance is 0.33 Btu/hr °F for the copper plate main heater.

3.3.3   TASK 2 TEST PROCEDURES

The twin test samples were installed in the test rig and the spacing between the hot and cold plates was carefully adjusted to provide the specified sample thickness by using precision gage blocks. For all tests, one particular face of each sample was maintained at approximately

70°F. Therefore, with environmental boundary temperatures of $\approx 175^{\circ}$ and $\approx 280^{\circ}$F, the 70° face of the sample was installed adjacent to the cold plate; for environmental temperatures of -100°F and -320°F, the samples were reversed so that the heater plate would maintain the 70° face temperature.

After pumping down the chamber to the desired pressure, the cold plate fluid was circulated through the coils until the desired cold plate temperature was attained. The initial setting of the main heater power was calculated using an estimated value of the effective sample conductivity. After reaching the desired heater plate temperature, adjustments in the main heater power were made to decrease the rate of change in heater plate temperature with time. This adjustment is calculated by measuring the observed rate of change in temperature and by evaluating the increase or decrease in power required to compensate for it. By knowing the heat capacity of the aluminum heater plate (from test, $W C_p = 0.279$ watt-hr/$^{\circ}$F), the power adjustment ΔP is approximately determined from:

$$\Delta P = W C_p \frac{d\,\overline{T}}{d\,t} \quad \text{measured}$$

where $d\,\overline{T}$ is the rate of mainheater plate temperature change with time. Figure 3-7 shows an example of such data.

Equilibrium conditions were considered to be achieved when the rate of heater plate temperature drift was less than 0.125°F per hour. With the guard heater controller adjusted to maintain a small difference between the main and guard heaters, equilibrium was considered to be achieved if the temperature differential was less than $\pm 0.30^{\circ}$F, which represents about a 99 percent heat balance. In order to obtain the preceding equilibrium conditions a minimum of six hours was required to establish thermal gradients within the material samples. Once the gradients were established and equilibrium was achieved, data was recorded for a minimum of two hours for use in the evaluation of effective conductivity.

The total heat transfer, Q (Btu/hr), conducted through the samples of insulation material is evaluated from the following heat balance for the heater plate:
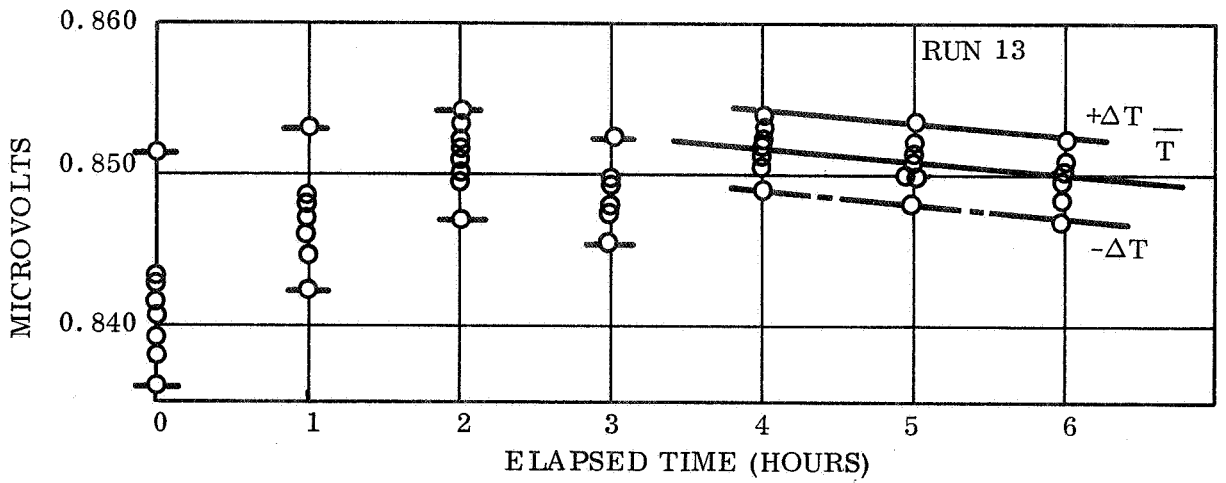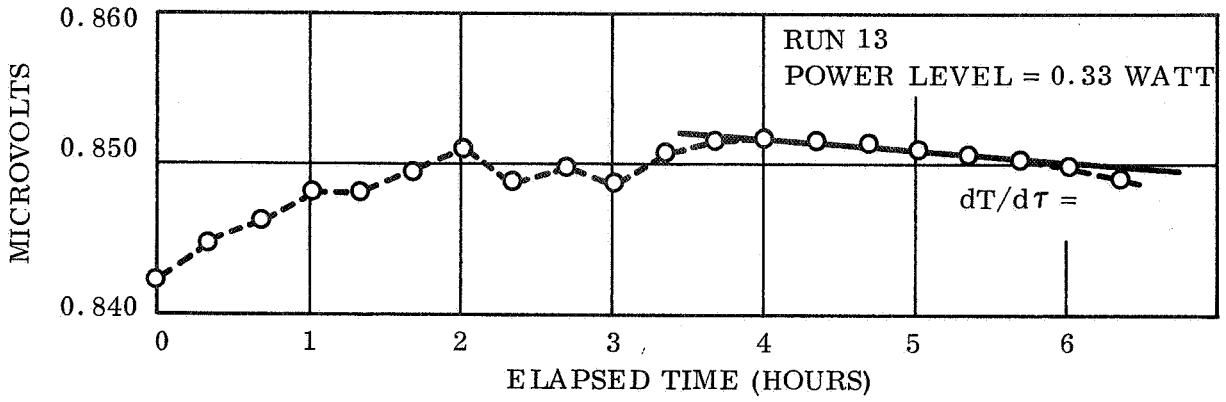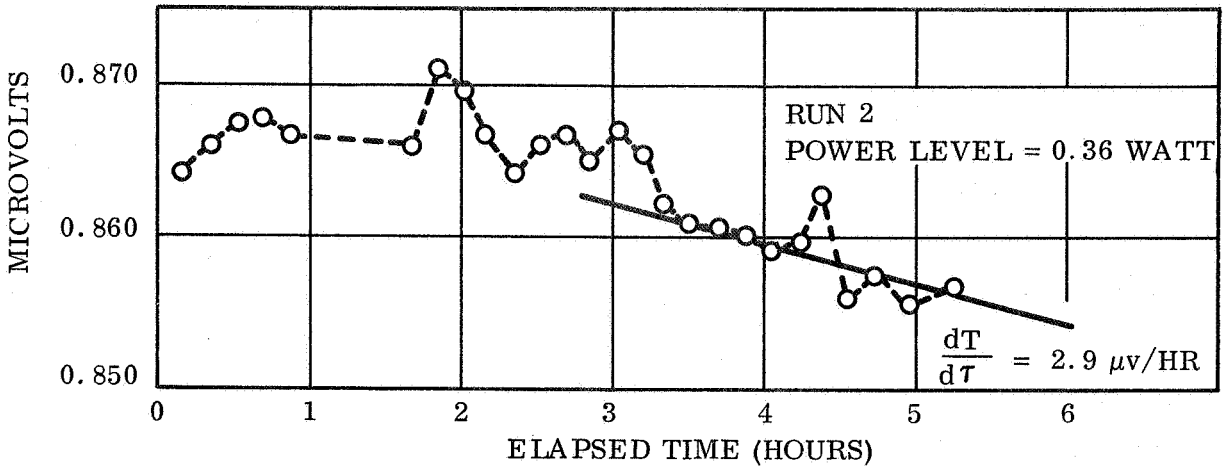
Figure 3-7. Typical Heater Plate Temperature - Time Histories

$$P_e = h_g(T_h - T_g) + Q/(3.412 \text{ Btu/watt-hr}) + WC_p\frac{d\overline{T}}{dt}$$

| Electrical Heat In | Heat Out Through Guard | Heat Out Through Insulation | Heat to Raise Heater Plate Temperature |

where: P_e = measured electrical power, watts

h_g = effective conductance between main and guard heaters = 0.096 watt/$^\circ$F

T_h = average main heater temperature, $^\circ$F

T_g = average guard heater temperature, $^\circ$F

WC_p = heat capacity of main heater, 0.279 $\frac{\text{watt-hr}}{^\circ\text{F}}$

$d\overline{T}/dt$ = rate of heater plate temperature change, $^\circ$F/hr

Using the measured quantities to solve the heat balance equation for Q, the effective conductivity of the insulation material is found from:

$$K = \frac{Q\,\Delta X}{A(T_h - T_c)}$$

where: K – effective conductivity, $\frac{\text{Btu-ft}}{\text{hr} - \text{ft}^2 - ^\circ\text{F}}$

Q – heat transfer, Btu/hr

Δx – sample thickness, ft

A – sample planform area, ft^2

T_h – heater plate temperature, $^\circ$F

T_c – cold plate temperature, $^\circ$F

The conductance of the material is determined by eliminating the sample thickness from the equation. Inasmuch as the density of a multilayer configuration is dependent on the sample thickness, and the heat transfer does not vary linearly with thickness, the conductance is a more realistic description of the thermal performance than the conductivity.

In the course of the Task 2 work, the procedures were improved in an effort to enhance the resolution of the data. The changes that were made do noticeably affect the consistency and the reliability of the results as the tests progressed chronologically. Some of the changes that were made are described in the following paragraphs, together with the reasons for deviation in procedure and the ensuing results.

Initially, with a temperature controlled, intermittent power input to the main heater, the cyclic temperature history made it very difficult to accurately evaluate the mean temperature and the mean temperature drift. Therefore, an iterative procedure was initiated to provide a constant power input. This procedure provided better accuracy in the determination of average heater plate temperatures, average variations in temperature differences between main and guard heaters, and the total power input to the main heater.

Later, a procedure was adopted to measure all heater plate temperatures more accurately on a K-3 precision potentiometer. Although the required accuracy of the absolute temperature level does not warrant such measurements, the small temperature drifts ($\approx 0.2^{O}$F/hr) can significantly affect the conductance measurements at the low heat transfer rates. Also, the K-3 potentiometer provided an accurate monitor of the thermal gradients in the heater plate, which clearly demonstrate the approach to thermal equilibrium. A comparison of heater plate temperature histories with and without the K-3 temperature measurements is shown in Figure 3-7. This comparison shows two typical runs at about the same heater plate temperature and power levels. The determination of temperature drift is shown to be more accurate using the K-3 potentiometer system. Time and temperature variations in the plate are also shown in Figure 3-7, to demonstrate the approach to thermal equilibrium. It can be noted that the variation in maximum to minimum temperature of about 5 to 6 microvolts does not change over the final two hours. The variation of about 6 microvolts represents approximately the accuracy of the absolute temperature as measured by uncalibrated chromel-alumel thermocouples, and the stability of this variation represents the approach to thermal equilibrium.

A third change in the test procedure was to monitor the thermal transients between the main and guard heaters with the K-3 precision potentiometer. This procedure allowed a more accurate evaluation of the mean temperature difference. The continuous observation over several cycles at each data recording period provided peak-to-peak variation information to evaluate the mean value rather than a random sampling, as would be obtained by using an automatic readout system.

Figure 3-8 shows the test apparatus with guard heater insulation. Figure 3-9 shows the test area.
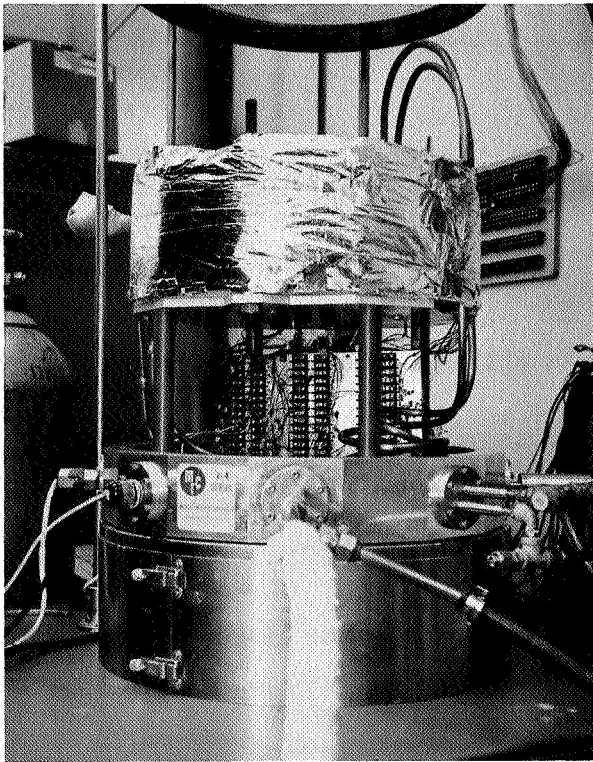

Figure 3-8. Test Apparatus with
Guard Heater Insulation

Figure 3-9. Test Area

3.4 POTENTIAL ERRORS

The measurement of extremely small heat flows in this experimental program, in which heat leaks to or from the surrounding environment can be a significant portion of the heat flow through the test sample, introduces the problem of potential errors. Although there was a continuous effort to minimize errors, it is felt necessary to list and describe potential errors, even though most such errors were insignificant relative to the measurments being performed. Such errors can be related to either of the following:

a. Test apparatus design

b. Measurements and control

The potential errors and their possible effects on the results are discussed in this section, with emphasis on the former. Effects on test results have been discussed in Section 2.

3.4.1 TEST APPARATUS DESIGN

The potential errors introduced by test apparatus design can be due to uncompensated heat sources or heat leaks, test apparatus nonsymmetry, or plate alignment.

Since the heater and guarding system permits compensation of losses, no errors are expected. The edges of the cold and heater plate guard are protected from losses by a circumferential insulation blanket, eliminating any significant errors in this direction. Thermal symmetry is checked by the distributed thermocouples.

The remaining potential error sources include heater and cooling plate alignment, since it can be assumed that the previous sources of error are negligible. The procedure used in the alignment of the plates is consistent from test to test, so that sources of error again are negligible. Thus, an error of 0.003 inch on the smallest spacing used in this program, 3/32 inch, represents about a 3 percent potential error in conductivity.

The major source of potential error, however, is due to the nonflatness of the copper heater plate used during the work of Task 1. The 8 1/4 inch square main heater section and corresponding cold plate sections were checked for flatness deviation prior to the start of Task 1. It was found that the cold plates were flat within ±0.006 inch maximum and ± 0.003 inch average. However, the heater plate was found to be nonflat by as much as ±0.025 inch locally and to have waviness of about ± 0.010 inch. While the cold plate flatness was within acceptable tolerances, the heater plate flatness was not.

Although repair in the form of machining or grinding was considered, it was not certain that such repair either would be successful or would not interfere with the embedded instrumentation. Since shop personnel could not give assurance of handling the instrumented heater plate without damage, it was decided to proceed with the test, while constructing a new heater plate.

We reasoned that, although the average potential flatness deviation error would be high, the relative error from layup to layup in Task 1 would be neglible, since the total sample thickness did not change. Thus, while the absolute thickness may be in error by as much as ± 25 mils, the relative thickness was approximately 0.325 ± 0.025 inch or ± 8 percent. While not desirable, the potential error was not unduly excessive for this type of measurement.

Near the conclusion of Task 1 tests, a new heater plate having flatness tolerances of ± 2 mils was installed for use in the remainder of Task 1 and for all Task 2 tests. Since Task 2 tests involved sample thickness variations, this change was beneficial as well as necessary. Thus, maximum potential thickness errors due to both plates now ranged from about ± 6 mils, or 6 percent for the smallest spacing of 3/32 inch, to 3 percent for the largest spacing tested.

3.4.3 MEASUREMENT AND CONTROL

The measurement and control of temperature and power input for the test rig represents a potential source of error. While it probably represents the largest such source, it is also the most controllable.

The heater power control during Task 1 was based on automatic, but intermittent, on-off control of the main heater. This technique was a potential source of errors when power was not on most of the time. Errors could be introduced as a result of timing tolerances, voltage fluctuations, and possible variation in heater resistance. Most of these potential errors were eliminated by changing to a manually controlled constant heater power technique. While this technique required a longer period initially to achieve equilibrium conditions, it resulted in better reproducibility of data. Measurement of voltage and current to the main heater was monitored to assure that there was no excessive drift in the regulated power supply. The digital voltmeter, used in this check, was in turn checked daily for maintenance of its calibration. In the few instances when equipment troubles developed, these procedures proved extremely beneficial.

The accuracy of the heat flow measurements through the insulation material under test also depends on the heat balance between the main and guard heaters, and on the possible temperature drift in the main heater. These corrections to the heat balance were kept small (from zero to approximately 5 percent) and therefore represented only a very small portion of the heat flow.

Potential errors involved in data processing or reduction also may be significant. Readouts were recorded to within the calibration accuracy of the readout instruments and this accuracy was carried through the data reduction. The significance of this procedure is that the accuracies involved are for relative rather than absolute measurements. For example, the accuracy of uncalibrated precision wire chromel-alumel thermocouples for absolute temperature measurements is $\pm 0.25^\circ F$, or about five microvolts at best, but relative measurements should be accurate to the calibration level of the recording instruments for wire from the same batch. The digital voltmeter records thermocouple outputs to be nearest microvolt, whereas the K-3 potentiometer can provide output measurements to the nearest tenth of a microvolt. Although the more precise measurement tolerances are well within the nominal accuracy of the thermocouple, the relative measurements to less than $0.1^\circ F$ do provide more accurate tracking of thermal transients and eliminate any significant potential errors in the test results.

SECTION 4

REFERENCES

1. E. Fried, and G. Karp, "Measurement of Thermal Conductance of Multilayer and Other Insulation Materials," General Electric Co. Report 66SD4207, Contract NAS 9-3685, January 1966.

2. G. Karp and C. S. Lankton, "A Guarded Hot Plate Thermal Conductivity Apparatus for Multilayer Cryogenic Insulation," ASTM Publication STP 411, 1967.

3. W. L. Gill, J. C. Poradek and F. Burgett, "Summary of the State of the Art of Superinsulation for Space Suits," Part of RFP BG 721-23-7-357P, 1967.

4. M. L. Minges, "Thermal Insulation for Aerospace Applications," ASD-TDR-63-699, 1963.

5. "Basic Investigations of Multilayer Insulation Systems," NASA CR-54191, Arthur D. Little, Inc., October 30, 1964.

6. "Advanced Studies on Multilayer Insulation Systems," NASA CR 54929, Contract NAS 3-6283, Arthur D. Little Inc., June 1, 1966.

7. "Planetary Vehicle Thermal Insulation Study," Phase One Summary Report, JPL Contract 951537, General Electric Co. Presentation, April 1967, GE Report 67SD4289.

8. E. R. Streed, G. R. Cunnington, and C. A. Zierman, "Performance of Multilayer Insulation Systems for the 300° to 800°K Temperature Range," AIAA Paper 65-663, AIAA Thermophysics Spec. Conf. September 1965.

9. J. J. Brogan et al., "Design of High Performance Insulation Systems," Vol. V, LMSC-A742593-1, Contract No. NAS-8-11347, 1965.

10. E. Fried and M. J. Kelley, "Thermal Conductance of Metallic Contacts in a Vacuum," in Thermophysics and Temperature Control of Spacecraft, ed. by G. B. Heller, Academic Press, 1967, p. 697.